Synchronized oscillations in a mathematical model of segmentation in zebrafish

2012 Nonlinearity 25 869

(http://iopscience.iop.org/0951-7715/25/4/869)

IOP PUBLISHING NONLINEARITY

Nonlinearity **25** (2012) 869–904 doi:10.1088/0951-7715/25/4/869

Synchronized oscillations in a mathematical model of segmentation in zebrafish

Kang-Ling Liao[1], **Chih-Wen Shih**[1,3] **and Jui-Pin Tseng**[2]

[1] Department of Applied Mathematics, National Chiao Tung University, Hsinchu 300, Taiwan
[2] Department of Applied Mathematics, National Pingtung University of Education, Pingtung 900, Taiwan

E-mail: cwshih@math.nctu.edu.tw

Received 30 July 2010, in final form 29 August 2011
Published 28 February 2012
Online at stacks.iop.org/Non/25/869

Recommended by J A Sherratt

Abstract

Somitogenesis is a process for the development of somites which are transient, segmental structures that lie along the anterior–posterior axis of vertebrate embryos. The pattern of somites is governed by the segmentation clock and its timing is controlled by the clock genes which undergo synchronous oscillation over adjacent cells in the posterior presomitic mesoderm (PSM). In this paper, we analyze a mathematical model which depicts the kinetics of the zebrafish segmentation clock genes subject to direct autorepression by their own products under time delay, and cell-to-cell interaction through Delta–Notch signalling. Our goal is to elucidate how synchronous oscillations are generated for the cells in the posterior PSM, and how oscillations are arrested for the cells in the anterior PSM. For this system of delayed equations, an iteration technique is employed to derive the global convergence to the synchronous equilibrium, which corresponds to the oscillation-arrested. By applying the delay Hopf bifurcation theory and the center manifold theorem, we derive the criteria for the existence of stable synchronous oscillations for the cells at the tail bud of the PSM. Our analysis provides the basic parameter ranges and delay magnitudes for stable synchronous, asynchronous oscillation and oscillation-arrested. We exhibit how synchronous oscillations are affected by the degradation rates and delays. Extended from the analytic theory, further numerical findings linked to the segmentation process are presented.

Mathematics Subject Classification: 37N25, 34K18, 92D15

(Some figures may appear in colour only in the online journal)

[3] Author to whom any correspondence should be addressed.

1. Introduction

Somites are transient, segmental structures that lie along the anterior–posterior axis of vertebrate embryos. They arise from the presomitic mesoderm (PSM) repeatedly and develop into the vertebrae, rib and tail, under further differentiation. This whole process, termed somitogenesis, is controlled by the segmentation clock which comprises a multicellular genetic network of oscillators acting in the PSM to drive periodic expression of the cyclic genes [11, 18, 22, 26, 28]. Somitogenesis involves tight gene regulation in both space and time. The cyclic genes express synchronous oscillations in the tail bud of the PSM. Underlying the morphogenetic rhythm of somitogenesis, repeated waves of oscillatory gene expression propagate from posterior to anterior; the oscillations then slow down and finally arrest and cells are formed into somites. Key cycling genes for the segmentation clock have been identified, namely, *Hes*1 and *Hes*7 in mouse, *hairy*1 and *hairy*2 in chick and *her*1 and *her*7 in zebrafish [6, 18, 27]. In particular, the oscillation period of the cyclic genes in the tail bud of zebrafish is about 30 min, which matches the time taken to generate a somite [17].

Theoretical modelling of somite segmentation starts from a 'clock and wavefront' model proposed by Cooke and Zeeman [5]. The interface between the gene expression oscillation and the oscillation-arrested is called 'wavefront' which determines where the somites form. It has been discovered in experiments that the signalling molecule fibroblast growth factor (FGF) regulates the differentiation of PSM cells [9, 19, 38]. FGF8 is only transcribed at the posterior tip of the embryo and spreads anteriorly with gradient. In addition, there exists a threshold for FGF8: if the FGF8 is smaller than the threshold, then the oscillation starts to slow down and cells will then form into somites. Based on the experimental observations of FGF8 [7, 8, 13, 17], Baker *et al* [1] performed a mathematical study on the pattern formation mechanism for somites under moving gradient of FGF8 expression along the anterior–posterior axis of vertebrate embryos. The segmentation clock genes were not taken into account in that model.

While somite oscillators in chick and mouse are considered more complicated than fish, zebrafish has been a standard model organism for investigating somitogenesis. For zebrafish, *her*1 and *her*7 are the genes that satisfy the conditions to be central components of the somitogenesis oscillator. Modelling the kinetics of segmentation clock genes for zebrafish was proposed by Lewis who advocated that direct autorepression of *her*1 and/or *her*7 by their own products provides a mechanism for the intracellular oscillator. Accordingly, negative feedback with time delay in gene regulation was modelled to generate the oscillatory gene expression [21]. In zebrafish, the synchronization is realized by intercellular interaction via Delta–Notch signalling. These oscillatory genes, *her*1, *her*7, and the Notch ligand DeltaC all belong to the Notch signalling pathway.

Notch signalling pathway has been shown to play a critical role in somitogenesis in a number of experiments. The hypotheses of the Notch signalling pathway include oscillation-generator, boundary-formation, synchronization and polarity-formation [22, 25]. For zebrafish, synchronization and polarity-formation are the only functions of Notch signalling pathway in the tail bud and the somites, respectively. This was justified in [22, 25] via the mutants caused by blocking the Notch signalling pathway through adding the chemical inhibitor DAPT or overactivating the Notch signalling pathway by driving the expression of NICD (activated form of Notch). In mathematical modelling, it is assumed that NICD generated is proportional to the amount of Delta protein in the neighbouring cells. Hence, one still takes into account the expressions of *her*1, *her*7 and *delta* genes to investigate the function of Notch signalling pathway in zebrafish.

In this investigation, we aim at establishing analytical theories for the collective behaviour in the cell–cell kinetic model for the somitogenesis clock genes in zebrafish. We shall consider the homodimer system and take *her* gene as either *her*1 or *her*7; the two neighbouring cells interact through Delta–Notch signalling with delay. Let $x_1,\ x_2,\ x_3,\ x_4$ (respectively, $y_1,\ y_2,\ y_3,\ y_4$) represent the concentrations of *her* mRNA, Her protein, *delta* mRNA and Delta protein of the first cell (respectively, the second cell), respectively. The kinetics of these genes evolve according to the following equations:

$$\begin{aligned}
\dot{x}_1(t) &= g_{\mathrm{H}}(x_2(t-\tau_1), y_4(t-\tau_1)) - d_1 x_1(t)\\
\dot{x}_2(t) &= a_2 x_1(t-\tau_2) - d_2 x_2(t)\\
\dot{x}_3(t) &= g_{\mathrm{D}}(x_2(t-\tau_3)) - d_3 x_3(t)\\
\dot{x}_4(t) &= a_4 x_3(t-\tau_4) - d_4 x_4(t)\\
\dot{y}_1(t) &= g_{\mathrm{H}}(y_2(t-\tau_1), x_4(t-\tau_1)) - d_1 y_1(t)\\
\dot{y}_2(t) &= a_2 y_1(t-\tau_2) - d_2 y_2(t)\\
\dot{y}_3(t) &= g_{\mathrm{D}}(y_2(t-\tau_3)) - d_3 y_3(t)\\
\dot{y}_4(t) &= a_4 y_3(t-\tau_4) - d_4 y_4(t).
\end{aligned} \tag{1.1}$$

Herein, the first equation describes the evolution of *her* mRNA, with its first and second terms depicting the transcription and the degradation (with rate d_1), respectively. The second equation depicts the kinetics of Her protein, where the first and second terms express the translation with protein synthesis rate a_2 per mRNA molecule, and the degradation (with rate d_2), respectively. Similar interpretations apply to *delta* mRNA in the third equation and Delta protein on the cell membrane in the fourth equation of (1.1). $\tau_1,\ \tau_2,\ \tau_3,\ \tau_4$ are positive numbers which represent the time delays, incurred in the following processes:

$$\begin{aligned}
&\tau_1 = \tau_{mh} : \textit{her} \text{ gene transcription},\\
&\tau_2 = \tau_{ph} : \textit{her} \text{ gene translation},\\
&\tau_3 = \tau_{md} : \textit{delta} \text{ gene transcription},\\
&\tau_4 = \tau_{pd} : \textit{delta} \text{ gene translation and delivery to cell membrane.}
\end{aligned}$$

The functions g_{H} and g_{D} relate the transcription initiation rates to *her* and *delta* protein concentrations, respectively,

$$g_{\mathrm{H}}(u,v) = k_{\mathrm{H}} \frac{1 + b\frac{v}{P_{D_0}} + \nu}{1 + b\frac{v}{P_{D_0}} + \nu + \frac{u^2}{P_0^2}}, \qquad \text{for } u, v \geqslant 0, \tag{1.2}$$

$$g_{\mathrm{D}}(u) = \frac{k_{\mathrm{D}}}{1 + \frac{u^2}{P_0^2}}, \qquad \text{for } u \geqslant 0, \tag{1.3}$$

where k_{H} (respectively, k_{D}) is the maximal synthesis rate of *her* (respectively, *delta*) mRNA; P_0 (respectively, P_{D_0}) is the critical number of molecules of Her (respectively, Delta) protein per cell. In addition, $b = 1$ corresponds to the normal functioning of Notch signalling pathway; $b = 0$ represents the blockade of Notch signalling pathway (by adding DAPT); $\nu > 0$ means adding NICD to over-express the Notch signalling pathway. Since we only consider normal segmentation, we take $b = 1$ and $\nu = 0$ throughout this paper. Note that the Delta protein of the neighbouring cell stimulates the expression of *her* mRNA, as indicated in function g_{H}.

System (1.1) describes the kinetics of the gene expressions of two cells in contact; the locations of these two cells are regarded as fixed. The first four and last four equations are

coupled in a symmetric manner through the first and the fifth equations. We are interested in seeing the collective behaviour of the coupled-cell system (1.1) corresponding to various combinations of parameters and delay magnitudes. In particular, we shall investigate how synchronous oscillation and oscillation-arrested are achieved in this system. By *synchronous periodic solution*, we mean a periodic solution of (1.1) with $x_i(t) = y_i(t)$, $i = 1, 2, 3, 4$. If a synchronous periodic orbit is stable, then we say that the system admits (stable) *synchronous oscillation*. We will also address asynchronous or anti-phase oscillation which is related to mutation of segmentation. The parameter and delay magnitudes which yield synchronous oscillations and clock-wave formation are important in understanding the models and the defects of somitogenesis. As pointed out in [34], it is not obvious how synchronized oscillations are achieved via Delta–Notch signalling, as Delta proteins stimulate the expression of the *her* mRNA in neighbouring cells via Notch receptors, but the active expression of *her* in these cells suppresses the *delta* gene within them. Hence, how synchronization can be achieved, while sustaining the oscillation, requires a careful and detailed analysis in the study of somitogenesis models.

Synchronized oscillations for the *her*1/*her*7 heterodimer oscillator model and the homodimer oscillator based on *her*1 or *her*7 (system (1.1)) with a different transcription function g_{H} have been investigated numerically in [21]. It was indicated therein that the behaviour for *her*1/*her*7 heterodimer oscillator model is in general similar to that of a homodimer oscillator based on *her*1 or *her*7 alone. On the other hand, function g_{H} in (1.2) was adopted in [25] to describe the mutant caused by the absence or over-expression of Notch signalling. This modified form of g_{H} has the advantage that it can be reduced to the decoupled (single-cell) model when $b = 0$. However, if the cells are coupled (i.e. $b \neq 0$), then the dynamics for the system with either g_{H} are quite similar. Since our goal is to see how the Notch signalling promotes the synchronization, we only consider normal somite formation, and hence, the Notch signalling should be present. While the main focus is on system (1.1) in this work, our approach can be extended to treat the heterodimer model and systems with general transcription functions g_{H} and g_{D}.

Mathematical analysis truly confirms the dynamics of the considered systems, and hence provides a solid ground for comparison among various models and further extensions. The stability of nontrivial steady state and periodic orbit through the Hopf bifurcation theory for Lewis's single-cell model has been studied in [10]. Bifurcation analysis for the oscillatory gene expressions of other single-cell models was reported in [36, 37]. Analytic results on how synchronous oscillations between adjacent cells are achieved have been lacking, to the best of our knowledge. How delays affect the collective behaviour and oscillation in biological clocks has been an interesting issue to be tackled [16]. Yet, nonlinear systems with several components and multiple delays make mathematical analysis a difficult task [3, 31]. An effective way to analyze the characteristic equation which contains exponential functions, is to allocate the purely imaginary eigenvalues and compute the exchange of stability for the equilibrium as the first step. In applying the delay Hopf bifurcation theory, the computation in determining the direction and stability of bifurcated periodic orbit through the center manifold theory and the normal form theory is rather involved [36]. On the other hand, while stable synchronous periodic orbit is local dynamics, ruling out possible oscillation as an indication of oscillation-arrested requires a global result. Our analytic approach in concluding the regimes of the synchronous oscillation and oscillation-arrested is especially illuminating for biological systems with many parameters and multiple delays. Our investigation sheds light on certain important issues; for example, that large coupling strength benefits the synchronous oscillation, asserted in [28], actually also depends on appropriate magnitudes of degradation rates and delays.

The binding and dissociation of a gene protein to and from its site on DNA are stochastic processes. The deterministic system (1.1) is, in fact, modelled under the assumption that the random flickering behaviour of *her*1 and *her*7 can be replaced by their instantaneous time average. It was observed in [21] that the noisy system oscillates in the same way as the deterministic system, if the protein synthesis is at the full normal rate; therein, further numerical observation on the oscillations for the noisy system when the protein synthesis is attenuated was also reported. The effects from noise on segmentation have also been studied numerically in [2, 24, 28, 33, 35].

There were some extensions of Lewis's model. Her13.2 has been discovered to interact with clock proteins and control the rate of oscillation in zebrafish [19, 32]. Cinquin [4] proposed a multicellular delay system for zebrafish somitogenesis that involves heterodimerization of clock proteins Her1 and Her7, with protein Her13.2, to model the posterior-to-anterior slowing of oscillation rate, which leads to formation of clock-wave. Campanelli and Gedeon [2] generalized Lewis's model to a system with two different genetic control mechanisms to initiate the gene-expression wave, one on the number of clock protein transcription binding sites, the other on differential decay rates for clock protein monomers and dimers.

In the somitogenesis, time delays which have been estimated in the range of tens of minutes in cell culture are due to synthesis and trafficking of macromolecules in cells. Modelling with delays raises some mathematical technicality in differential equations. Replacing the time delay by taking into account certain intermediate process in the cell, namely, the translocation of Her protein from cytoplasm to nucleus, an ODE model has been studied in [33, 34]. Therein, Michaelis–Menten type reaction for the degradation and more general transcription function with Hill coefficients were employed. The investigation was mainly based on numerical computations. In fact, in that ODE system, as some of those over ten parameters varies, the equilibrium value, the linearization and its eigenvalues all change, which make bifurcation analysis a difficult task.

Another modelling of vertebrate segmentation is to depict the phase dynamics of coupled oscillators, where each of the oscillators represents a cell or a group of synchronous cells in the PSM. It was shown that disruption of Delta–Notch intercellular coupling increases the period of zebrafish somitogenesis and the embryonic segment length. An instability resulting from decreased coupling delay time was predicted by the theory of phase oscillator and justified by the experiments [16, 24]. A phase equation depicting the peak gene expression in the travelling wave for a lattice system of ODEs was discussed in [33]. On the one hand, the parameters in the kinetic models are more difficult to measure than those for the phase oscillators *in vivo* [12, 16, 34]. On the other hand, those phase models are built under certain assumptions; how they are linked to the solution behaviour of the kinetic equations which depict the interaction of cyclic genes, such as (1.1), remains to be investigated. This present work hopes to provide a basis for this linkage. Our analytic theory not only delineates qualitatively how the degradation rates, the other focal parameters and delays affect synchronous oscillations, but also provides the parameter regimes for oscillation-arrested, synchronous and asynchronous oscillations.

For mouse, the oscillating network of signalling genes underlying the segmentation clock is more complex. It was reported through experiments by Dequéant and coworkers [6] that the inhibitors of the Notch, FGF and Wnt signalling pathways are involved in the segmentation clock. In addition, numerical simulation on an ODE model for Notch, FGF and Wnt signalling pathways which contain the inhibitors discovered in [6], was performed to investigate the oscillation and the interactions among these three pathways in [13]. On the other hand, delay models for gene regulation of Axin2, Hes1 and Lfng, which belong to the Notch and Wnt signalling pathway, were employed to investigate the segmentation clock in mouse and chick in [29].

The paper is organized as follows. In section 2, we study the positive invariance of the considered domain and the dissipative property for system (1.1), for the validity of the model equations. We then show the existence of a synchronous equilibrium and apply an iteration technique developed in [30, 31] to derive the global convergence to the synchronous equilibrium. We regard this regime of parameters as the one for oscillation-arrested which corresponds biologically to the formed somites. Although there are other proteins involved in slowing down the oscillation, we interpret that these effects are reflected in altering the parameters, such as degradation rates, of the system. In section 3, we employ the delay Hopf bifurcation theorem to prove the existence of synchronous periodic solutions and use the center manifold theorem and the normal form method to analyze the stability of the bifurcated periodic solutions. In section 4, we summarize the collective behaviour of the coupled system (1.1), and give some numerical simulations to demonstrate our analytic results. In section 5, the paper ends with a conclusion.

2. Global convergence to steady state

In this section, we first examine the basic properties for system (1.1) to ensure that it is suitable to model gene regulation. We then show that (1.1) has a synchronous equilibrium $\bar{\mathbb{X}}$. A criterion for global convergence to $\bar{\mathbb{X}}$ is then derived.

For the coupled system (1.1) with four time delays $\tau_1, \tau_2, \tau_3, \tau_4$, in this paper, we consider the evolution $\Psi(t, \phi)$ of (1.1) from initial condition $\phi = (\phi_1, \ldots, \phi_8) \in \mathcal{C}([-\tau_M, 0], \mathbb{R}^8_+)$ at initial time $t_0 = 0$, where

$$\tau_M := \max\{\tau_1, \tau_2, \tau_3, \tau_4\}, \qquad \mathbb{R}^8_+ := \{(x_1, \ldots, x_4, y_1, \ldots, y_4) |\, x_i, y_i \geqslant 0,\ i = 1, \ldots, 4\}.$$

Let $\mathbb{X}(t; \phi)$ denote the solution induced from (1.1), which is defined by $\mathbb{X}(t + \theta; \phi) = \Psi(t, \phi)(\theta)$, $\theta \in [-\tau_M, 0]$, for $t > 0$. We further denote $\mathbb{X}(t) = (\boldsymbol{x}(t), \boldsymbol{y}(t)) = \mathbb{X}(t; \phi) = (\boldsymbol{x}(t; \phi), \boldsymbol{y}(t; \phi))$, where $\boldsymbol{x} = (x_1, x_2, x_3, x_4)$, $\boldsymbol{y} = (y_1, y_2, y_3, y_4)$, when ϕ is not specified. To ensure that (1.1) is proper in modelling the gene regulation, one first needs to ensure that the solution $\mathbb{X}(t; \phi)$ is always nonnegative, for any $\phi \in \mathcal{C}([-\tau_M, 0], \mathbb{R}^8_+)$.

Proposition 2.1. *$\mathcal{C}([-\tau_M, 0], \mathbb{R}^8_+)$ is positively invariant for system (1.1).*

Proof. We shall show that $x_i(t) \geqslant 0$, $y_i(t) \geqslant 0$, $i = 1, 2, 3, 4$, for solution $\mathbb{X}(t)$ evolved from arbitrary $\phi \in \mathcal{C}([-\tau_M, 0], \mathbb{R}^8_+)$. Let I be the maximal interval of existence for solution $\mathbb{X}(t)$. First,

$$\dot{x}_3(t) = -d_3 x_3(t) + g_{\mathrm{D}}(x_2(t - \tau_3)) > -d_3 x_3(t), \tag{2.1}$$

for all $t \in I$, since $g_{\mathrm{D}}(u) = k_{\mathrm{D}}/(1 + u^2/P_0^2) > 0$, for any u. It follows that $x_3(t) \geqslant 0$, for all $t \in I$, through comparison arguments. Similarly, we can show that $y_3(t) \geqslant 0$, for all $t \in I$, by the symmetry of system (1.1). With $x_3(t) \geqslant 0$ for all $t \in I$, we use similar argument to derive $x_4(t), y_4(t), x_1(t), y_1(t), x_2(t), y_2(t) \geqslant 0$, for all $t \in I$, successively. □

We next derive the existence of global attracting set for system (1.1).

Proposition 2.2. *There exists a closed and bounded set $\mathcal{Q} = \Pi_{i=1}^4 Q_i \times \Pi_{i=1}^4 Q_i \subset \mathbb{R}^8_+$, such that $\mathbb{X}(t; \phi)$ converges to $\mathcal{Q}$ for arbitrary $\phi \in \mathcal{C}([-\tau_M, 0], \mathbb{R}^8_+)$, where Q_i are defined by*

$$Q_1 = [\check{q}_1, \hat{q}_1] := [0, k_{\mathrm{H}}/d_1], \qquad Q_2 = [\check{q}_2, \hat{q}_2] := [0, a_2 k_{\mathrm{H}}/(d_1 d_2)],$$
$$Q_3 = [\check{q}_3, \hat{q}_3] := [\check{c}_3/d_3, k_{\mathrm{D}}/d_3], \qquad Q_4 = [\check{q}_4, \hat{q}_4] := [a_4 \check{c}_3/(d_3 d_4), a_4 k_{\mathrm{D}}/(d_3 d_4)]$$

and

$$\check{c}_3 := \frac{k_{\mathrm{D}} P_0^2}{P_0^2 + (\frac{a_2 k_{\mathrm{H}}}{d_1 d_2})^2}. \tag{2.2}$$

Proof. The assertion follows from estimating $\mathrm{d}x_i/\mathrm{d}t, \mathrm{d}y_i/\mathrm{d}t$ of system (1.1), and hence $x_i(t)$, $y_i(t)$, successively. From the definition of functions g_{H} and g_{D}, we have

$$0 < g_{\mathrm{H}}(u, v) \leqslant k_{\mathrm{H}}, \qquad 0 < g_{\mathrm{D}}(u) \leqslant k_{\mathrm{D}}, \qquad \text{for all } u, v \geqslant 0.$$

Let $\mathbb{X}(t;\phi) = \mathbb{X}(t) = (x_1(t), \ldots, x_4(t), y_1(t), \ldots, y_4(t))$ be the solution evolved from $\phi \in \mathcal{C}([-\tau_M, 0], \mathbb{R}^8_+)$. Note that, from proposition 2.1, $x_i(t), y_i(t) \geqslant 0$, for all $i = 1, 2, 3, 4$, $t \in I$. Hence,

$$-d_1 x_1(t) < \dot{x}_1(t) \leqslant -d_1 x_1(t) + k_{\mathrm{H}}, \qquad \text{for all } t \in I.$$

Consequently, $x_1(t)$ exists on $[0, \infty)$ and converges to $[0, k_{\mathrm{H}}/d_1] =: \tilde{Q}_1$, as $t \to \infty$. Subsequently, $x_2(t)$ also exists on $[0, \infty)$, with respect to the second component of system (1.1); in addition, for any $\epsilon > 0$, there exists some $t_1^\epsilon > 0$ such that

$$-d_2 x_2(t) \leqslant \dot{x}_2(t) \leqslant -d_2 x_2(t) + a_2 k_{\mathrm{H}}/d_1 + \epsilon, \qquad \text{for } t \geqslant t_1^\epsilon;$$

thus $x_2(t)$ converges to $[0, a_2 k_{\mathrm{H}}/(d_1 d_2) + \epsilon/d_2]$ for all $\epsilon > 0$, and hence converges to $[0, a_2 k_{\mathrm{H}}/(d_1 d_2)] =: \tilde{Q}_2$, as $t \to \infty$. By similar arguments, we can justify that $x_3(t)$ and $x_4(t)$ exist on $[0, \infty)$ and converge to $\tilde{Q}_3 := [0,\ k_{\mathrm{D}}/d_3]$ and $\tilde{Q}_4 := [0,\ a_4 k_{\mathrm{D}}/(d_3 d_4)]$, respectively. Moreover, we can also prove that $y_i(t)$ exists on $[0, \infty)$ and converges to set $\tilde{Q}_i$, $i = 1, 2, 3, 4$, by the symmetry of system (1.1).

So far, we have constructed a region, $\Pi_{i=1}^4 \tilde{Q}_i \times \Pi_{i=1}^4 \tilde{Q}_i$, to which every solution $\mathbb{X}(t)$ converges. We can continue to construct an attracting region smaller than $\Pi_{i=1}^4 \tilde{Q}_i \times \Pi_{i=1}^4 \tilde{Q}_i$, for system (1.1). Note that the convergence of $x_2(t)$ to $\tilde{Q}_2 = [0,\ a_2 k_{\mathrm{H}}/(d_1 d_2)]$ leads to that for any $\epsilon > 0$, there exists some $t_2^\epsilon > t_1^\epsilon$ such that $g_{\mathrm{D}}(x_2(t)) > k_{\mathrm{D}} P_0^2/[P_0^2 + (a_2 k_{\mathrm{H}}/(d_1 d_2))^2] - \epsilon =: \check{c}_3 - \epsilon$, for all $t \geqslant t_2^\epsilon - \tau_M > 0$. It follows from the third component of system (1.1) that

$$-d_3 x_3(t) + \check{c}_3 - \epsilon < \dot{x}_3(t) \leqslant -d_3 x_3(t) + k_{\mathrm{D}}, \qquad \text{for all } t \geqslant t_2^\epsilon.$$

Subsequently, $x_3(t)$ converges to $[\check{c}_3/d_3 - \epsilon/d_3, k_{\mathrm{D}}/d_3]$ for all $\epsilon > 0$, and hence converges to $[\check{c}_3/d_3, k_{\mathrm{D}}/d_3] =: Q_3 = [\check{q}_3, \hat{q}_3]$, as $t \to \infty$. By repeating the similar process, we can show that $x_4(t)$ converges to interval $Q_4 = [\check{q}_4, \hat{q}_4] := [a_4 \check{c}_3/(d_3 d_4),\ a_4 k_{\mathrm{D}}/(d_3 d_4)]$, as $t \to \infty$. Setting $Q_1 = [\check{q}_1, \hat{q}_1] := [0,\ k_{\mathrm{H}}/d_1]$ and $Q_2 = [\check{q}_2, \hat{q}_2] := [0, (a_2 k_{\mathrm{H}})/(d_1 d_2)]$, we also conclude that $x_i(t)$ converges to set Q_i, for $i = 1, 2$. Symmetrically, $y_i(t)$ converges to set Q_i, $i = 1, 2, 3, 4$. □

Remark 2.1. (i) By continuing the estimates in the proof of proposition 2.2 iteratively, we can confine the asymptotical behaviour of system (1.1) to smaller attracting set. For simplicity of presentation, we merely demonstrate the idea via two iteration steps. (ii) The assertion of proposition 2.2 indicates that every solution of (1.1) exists on $[0, \infty)$. (iii) Proposition 2.1 can be extended to conclude that the Delta protein is always positive, if its initial value is positive. Moreover, according to proposition 2.2, the Delta protein becomes larger than a positive value after certain time. This indicates that the Notch signalling is always present, if $b \neq 0$.

Next, we shall show that system (1.1) always admits one positive synchronous equilibrium. Herein, an equilibrium $(x_1^*, \ldots, x_4^*, y_1^*, \ldots, y_4^*)$ of (1.1) is *synchronous* if $x_i^* = y_i^*$, for $i = 1, 2, 3, 4$.

Proposition 2.3. *There exists a synchronous equilibrium point*

$$\bar{\mathbb{X}} = (\bar{\boldsymbol{x}}, \bar{\boldsymbol{x}}) = (\bar{x}_1, \bar{x}_2, \bar{x}_3, \bar{x}_4, \bar{x}_1, \bar{x}_2, \bar{x}_3, \bar{x}_4)$$

for system (1.1), where

$$\bar{x}_1 = \frac{d_2\bar{x}_2}{a_2}, \qquad \bar{x}_3 = \frac{k_{\mathrm{D}}P_0^2}{d_3(P_0^2+\bar{x}_2^2)}, \qquad \bar{x}_4 = \frac{a_4k_{\mathrm{D}}P_0^2}{d_3d_4(P_0^2+\bar{x}_2^2)},$$

and $\bar{x}_2$ is a positive solution to the equation:

$$p(\xi) := c_5\xi^5 + c_3\xi^3 - c_2\xi^2 + c_1\xi = a_2k_{\mathrm{H}}P_0^4(d_3d_4P_{D_0} + a_4k_{\mathrm{D}}), \tag{2.3}$$

and $c_5 = d_1d_2d_3d_4P_{D_0} > 0$, $c_3 = 2d_1d_2d_3d_4P_0^2P_{D_0} > 0$, $c_2 = a_2d_3d_4k_{\mathrm{H}}P_0^2P_{D_0} > 0$, $c_1 = d_1d_2P_0^4(d_3d_4P_{D_0} + a_4k_{\mathrm{D}}) > 0$.

Proof. Finding the synchronous equilibrium for (1.1) amounts to solving

$$\begin{aligned} &g_{\mathrm{H}}(x_2, x_4) - d_1x_1 = 0,\\ &a_2x_1 - d_2x_2 = 0,\\ &g_{\mathrm{D}}(x_2) - d_3x_3 = 0,\\ &a_4x_3 - d_4x_4 = 0. \end{aligned} \tag{2.4}$$

Then $(\bar{x}_1, \bar{x}_2, \bar{x}_3, \bar{x}_4)$ satisfies (2.4) if and only if

$$\bar{x}_1 = \frac{d_2\bar{x}_2}{a_2}, \qquad \bar{x}_3 = \frac{k_{\mathrm{D}}P_0^2}{d_3(P_0^2+\bar{x}_2^2)}, \qquad \bar{x}_4 = \frac{a_4k_{\mathrm{D}}P_0^2}{d_3d_4(P_0^2+\bar{x}_2^2)},$$

and $\bar{x}_2$ satisfies (2.3). Since $p(\xi) \to \infty$ as $\xi \to \infty$ and $p(0) = 0 < a_2k_{\mathrm{H}}P_0^4(d_3d_4P_{D_0} + a_4k_{\mathrm{D}})$, there exists a solution $\xi_0 > 0$ satisfying $p(\xi_0) = a_2k_{\mathrm{H}}P_0^4(d_3d_4P_{D_0} + a_4k_{\mathrm{D}})$. □

Note that every component of $\bar{\mathbb{X}}$ is positive. In the rest of this section, we shall discuss global convergence and synchronization. A criterion will be derived to yield both global synchronization and global convergence to the synchronous equilibrium point $\bar{\mathbb{X}}$ for system (1.1). To this end, we let $\tilde{\boldsymbol{x}}(t) = \boldsymbol{x}(t) - \bar{\boldsymbol{x}}$, $\tilde{\boldsymbol{y}}(t) = \boldsymbol{y}(t) - \bar{\boldsymbol{x}}$, and still denote $\tilde{\boldsymbol{x}}$, $\tilde{\boldsymbol{y}}$ by $\boldsymbol{x}$, $\boldsymbol{y}$ respectively. System (1.1) becomes

$$\begin{aligned} \dot{x}_1(t) &= -d_1x_1(t) + g_{\mathrm{H}}(x_2(t-\tau_1) + \bar{x}_2, y_4(t-\tau_1) + \bar{x}_4) - d_1\bar{x}_1,\\ \dot{x}_2(t) &= -d_2x_2(t) + a_2x_1(t-\tau_2),\\ \dot{x}_3(t) &= -d_3x_3(t) + g_{\mathrm{D}}(x_2(t-\tau_3) + \bar{x}_2) - d_3\bar{x}_3,\\ \dot{x}_4(t) &= -d_4x_4(t) + a_4x_3(t-\tau_4),\\ \dot{y}_1(t) &= -d_1y_1(t) + g_{\mathrm{H}}(y_2(t-\tau_1) + \bar{x}_2, x_4(t-\tau_1) + \bar{x}_4) - d_1\bar{x}_1,\\ \dot{y}_2(t) &= -d_2y_2(t) + a_2y_1(t-\tau_2),\\ \dot{y}_3(t) &= -d_3y_3(t) + g_{\mathrm{D}}(y_2(t-\tau_3) + \bar{x}_2) - d_3\bar{x}_3,\\ \dot{y}_4(t) &= -d_4y_4(t) + a_4y_3(t-\tau_4). \end{aligned} \tag{2.5}$$

We shall show that every solution converges to the origin for system (2.5). Consider an arbitrary solution $\mathbb{X}(t) = (x_1(t), \ldots, x_4(t), y_1(t), \ldots, y_4(t))$ of (2.5); then $\mathbb{X}(t)$ exists on $[0, \infty)$ according to remark 2.1(ii). As $x_i(t)$, $y_i(t)$ satisfy (2.5), by the mean value theorem, we have

$$\begin{aligned} \dot{x}_i(t) &= -d_ix_i(t) + w_i(t),\\ \dot{y}_i(t) &= -d_iy_i(t) + w_{i+4}(t), \end{aligned} \tag{2.6}$$

where $i = 1, 2, 3, 4$, and

$$
\begin{aligned}
w_1(t) &:= \frac{\partial g_{\mathrm{H}}}{\partial u}(u_1(t-\tau_1), v_1(t-\tau_1))x_2(t-\tau_1) + \frac{\partial g_{\mathrm{H}}}{\partial v}(u_1(t-\tau_1), v_1(t-\tau_1))y_4(t-\tau_1),\\
w_2(t) &:= a_2 x_1(t-\tau_2),\\
w_3(t) &:= \frac{\mathrm{d}g_{\mathrm{D}}}{\mathrm{d}u}(u_3(t-\tau_3))x_2(t-\tau_3),\\
w_4(t) &:= a_4 x_3(t-\tau_4),\\
w_5(t) &:= \frac{\partial g_{\mathrm{H}}}{\partial u}(\tilde{u}_1(t-\tau_1), \tilde{v}_1(t-\tau_1))y_2(t-\tau_1) + \frac{\partial g_{\mathrm{H}}}{\partial v}(\tilde{u}_1(t-\tau_1), \tilde{v}_1(t-\tau_1))x_4(t-\tau_1),\\
w_6(t) &:= a_2 y_1(t-\tau_2),\\
w_7(t) &:= \frac{\mathrm{d}g_{\mathrm{D}}}{\mathrm{d}u}(\tilde{u}_3(t-\tau_3))y_2(t-\tau_3),\\
w_8(t) &:= a_4 y_3(t-\tau_4),
\end{aligned}
$$

where $u_1(t-\tau_1)$ (respectively, $v_1(t-\tau_1)$, $u_3(t-\tau_3)$, $\tilde{u}_1(t-\tau_1)$, $\tilde{v}_1(t-\tau_1)$, $\tilde{u}_3(t-\tau_3)$) is between $x_2(t-\tau_1)+\bar{x}_2$ and $\bar{x}_2$ (respectively, $y_4(t-\tau_1)+\bar{x}_4$ and $\bar{x}_4$, $x_2(t-\tau_3)+\bar{x}_2$ and $\bar{x}_2$, $y_2(t-\tau_1)+\bar{x}_2$ and $\bar{x}_2$, $x_4(t-\tau_1)+\bar{x}_4$ and $\bar{x}_4$, $y_2(t-\tau_3)+\bar{x}_2$ and $\bar{x}_2$). Note that the solution $\mathbb{X}(t)$ of system (2.5) eventually converges to $\mathcal{Q}-\bar{\mathbb{X}} = \Pi_{i=1}^4 Q_i^* \times \Pi_{i=1}^4 Q_i^*$, where $Q_i^* := [\check{q}_i - \bar{x}_i, \hat{q}_i - \bar{x}_i]$, for $i = 1, 2, 3, 4$. Every component of (2.6) is of the form

$$\dot{x}(t) = -cx(t) + w(t), \tag{2.7}$$

where $c > 0$ is a constant and $w(t)$ is a continuous scalar function. For any $t \geqslant 0$, we denote

$$|w|^{\max}(t) := \sup\{|w(s)| : s \geqslant t\},\ |w|^{\max}(\infty) := \lim_{t\to\infty} |w|^{\max}(t).$$

It is not difficult to derive the following property; cf [30].

Lemma 2.4. *Every solution of (2.7) converges to an interval* $[-\tilde{\delta}, \tilde{\delta}]$, *where*

$$0 \leqslant \tilde{\delta} \leqslant |w|^{\max}(\infty)/c.$$

According to lemma 2.4, there exist eight intervals $I_i := [-\delta_i, \delta_i]$, $i = 1, \cdots, 8$, to which the ith component of $\mathbb{X}(t)$ converges respectively. Moreover,

$$
\begin{aligned}
&0 \leqslant \delta_i \leqslant |w_i|^{\max}(\infty)/d_i, \qquad \text{for } i = 1, \ldots, 4,\\
&0 \leqslant \delta_i \leqslant |w_i|^{\max}(\infty)/d_{i-4}, \qquad \text{for } i = 5, \ldots, 8.
\end{aligned}
$$

Next, we construct a sequence of nonnegative numbers $\{\delta_i^{(k)}\}_{k=1}^{\infty}$ through an iteration process to derive sharper estimates for δ_i, $i = 1, \ldots, 8$. We introduce

$$
\begin{aligned}
\rho_1 &:= \max\left\{\left|\frac{\partial g_{\mathrm{H}}(u, v)}{\partial u}\right| : u \in Q_2, v \in Q_4\right\},\\
\rho_2 &:= \max\left\{\left|\frac{\partial g_{\mathrm{H}}(u, v)}{\partial v}\right| : u \in Q_2, v \in Q_4\right\},\\
\rho_3 &:= \max\left\{\left|\frac{\mathrm{d}g_{\mathrm{D}}(u)}{\mathrm{d}u}\right| : u \in Q_2\right\}.
\end{aligned}
\tag{2.8}
$$

Proposition 2.5. *For each* $i = 1, \ldots, 8$, *there exists a sequence of nonnegative numbers* $\{\delta_i^{(k)}\}_{k=1}^{\infty}$ *with* $\delta_i^{(k)} \geqslant \delta_i$ *such that for each* k, *the* i*th component for the solution* $\mathbb{X}(t)$ *of system (2.5) converges to* $I_i^{(k)} := [-\delta_i^{(k)}, \delta_i^{(k)}]$, *as* $t \to \infty$, *and* $\delta_i^{(k)}$ *satisfies*

$$
\begin{aligned}
&0 \leqslant \delta_1^{(k)} = \delta_5^{(k)} := (\rho_1\delta_2^{(k-1)} + \rho_2\delta_4^{(k-1)})/d_1,\\
&0 \leqslant \delta_2^{(k)} = \delta_6^{(k)} := (a_2/d_2)\delta_1^{(k)},\\
&0 \leqslant \delta_3^{(k)} = \delta_7^{(k)} := (\rho_3/d_3)\delta_2^{(k)},\\
&0 \leqslant \delta_4^{(k)} = \delta_8^{(k)} := (a_4/d_4)\delta_3^{(k)},
\end{aligned}
\tag{2.9}
$$

where $\delta_2^{(0)} := \max\{|\check{q}_2 - \bar{x}_2|, |\hat{q}_2 - \bar{x}_2|\}$ *and* $\delta_4^{(0)} := \max\{|\check{q}_4 - \bar{x}_4|, |\hat{q}_4 - \bar{x}_4|\}$, $k \geqslant 1$, *and* ρ_i *are defined in (2.8).*

Proof. From lemma 2.4, $x_1(t)$ and $y_1(t)$ converge to intervals $[-\delta_1, \delta_1]$ and $[-\delta_5, \delta_5]$, as $t \to \infty$, respectively, where

$$0 \leqslant \delta_i \leqslant |w_i|^{\max}(\infty)/d_1, \qquad i = 1, 5.$$

Note that both $x_2(t)$ and $y_2(t)$ eventually converge to $Q_2^* = [\check{q}_2 - \bar{x}_2, \hat{q}_2 - \bar{x}_2]$, and both $x_4(t)$ and $y_4(t)$ eventually converge to $Q_4^* = [\check{q}_4 - \bar{x}_4, \hat{q}_4 - \bar{x}_4]$; therefore $u_1(t - \tau_1)$ and $\tilde{u}_1(t - \tau_1)$ eventually converge to Q_2 and $v_1(t - \tau_1)$ and $\tilde{v}_1(t - \tau_1)$ eventually converge to Q_4. Accordingly, for $i = 1, 5$,

$$\begin{aligned} |w_i|^{\max}(\infty) \leqslant\ & \rho_1 \max\{|\check{q}_2 - \bar{x}_2|, |\hat{q}_2 - \bar{x}_2|\} + \rho_2 \max\{|\check{q}_4 - \bar{x}_4|, |\hat{q}_4 - \bar{x}_4|\} \\ =:\ & \rho_1\delta_2^{(0)} + \rho_2\delta_4^{(0)}. \end{aligned}$$

We may say that $x_1(t)$ and $y_1(t)$ converge to the closed and bounded intervals $I_1^{(1)} := [-\delta_1^{(1)}, \delta_1^{(1)}] \supset I_1$ and $I_5^{(1)} := [-\delta_5^{(1)}, \delta_5^{(1)}] \supset I_5$, respectively, where $\delta_1^{(1)} = \delta_5^{(1)} := (\rho_1\delta_2^{(0)} + \rho_2\delta_4^{(0)})/d_1$. It then follows that for $i = 2, 6$,

$$\delta_i \leqslant |w_i|^{\max}(\infty)/d_2 \leqslant (a_2/d_2)\delta_1^{(1)},$$

since $|w_2(t)| = |a_2x_1(t - \tau_2)|$, $|w_6(t)| = |a_2y_1(t - \tau_2)|$, and thus $|w_i|^{\max}(\infty) \leqslant a_2\delta_1^{(1)}$, $i = 2, 6$. We then conclude that $x_2(t)$ and $y_2(t)$ converge to closed and bounded intervals $I_2^{(1)} := [-\delta_2^{(1)}, \delta_2^{(1)}] \supset I_2$ and $I_6^{(1)} := [-\delta_6^{(1)}, \delta_6^{(1)}] \supset I_6$, respectively, where $\delta_2^{(1)} = \delta_6^{(1)} := (a_2/d_2)\delta_1^{(1)}$. By continuing this process, we obtain (2.9). □

In the following theorem, with the help of proposition 2.5, we derive the condition for $\delta_i^{(k)}$ to converge to zero as $k \to \infty$, which yields $\delta_i = 0$, for $i = 1, \ldots, 8$.

Theorem 2.6. *System (1.1) achieves global convergence to the synchronous equilibrium point* $\bar{\mathbb{X}}$*; that is,* $x_i(t), y_i(t) \to \bar{x}_i$, *as* $t \to \infty$, $i = 1, 2, 3, 4$, *for solution* $(x_1(t), \ldots, x_4(t), y_1(t), \ldots, y_4(t))$ *of system (1.1), evolved from any initial condition in* $\mathcal{C}([-\tau_M, 0], \mathbb{R}_+^8)$, *if*

$$\rho_1a_2d_3d_4 + \rho_2\rho_3a_2a_4 < d_1d_2d_3d_4 =: \beta_4. \tag{2.10}$$

Proof. To justify the assertion, it suffices to show that $\delta_i^{(k)}$ converges to zero as $k \to \infty$ for all $i = 1, \cdots, 8$. From the iterative estimate in (2.9), we obtain

$$\begin{aligned} \delta_1^{(k)} &= (\rho_1\delta_2^{(k-1)} + \rho_2\delta_4^{(k-1)})/d_1 \\ &= \frac{\rho_1a_2}{d_1d_2}\delta_1^{(k-1)} + \frac{\rho_2a_4\rho_3a_2}{d_1d_4d_3d_2}\delta_1^{(k-1)} \\ &= \frac{\rho_1a_2d_3d_4 + \rho_2\rho_3a_2a_4}{d_1d_2d_3d_4}\delta_1^{(k-1)} \\ &=: \mathcal{R}\delta_1^{(k-1)}. \end{aligned}$$

Thus $\delta_1^{(k)} \to 0$, as $k \to \infty$, since $0 < \mathcal{R} < 1$, by (2.10). Subsequently, $\delta_i^{(k)} \to 0$, as $k \to \infty$, for $i = 2, \ldots, 8$, with respect to (2.9). □

Remark 2.2. (i) In fact, we can compute the upper bounds for the derivatives of g_{H} and g_{D}:

$$\begin{aligned}
0 \leqslant \left|\frac{\partial g_{\mathrm{H}}(u,v)}{\partial u}\right| &\leqslant \frac{2k_{\mathrm{H}}P_0^2 P_{D_0}\hat{q}_2(P_{D_0}+\hat{q}_4)}{P_0^4(P_{D_0}+\check{q}_4)^2} =: \hat{\rho}_1, \qquad \text{for } u \in Q_2, \quad v \in Q_4,\\
0 \leqslant \left|\frac{\partial g_{\mathrm{H}}(u,v)}{\partial v}\right| &\leqslant \frac{k_{\mathrm{H}}P_0^2 P_{D_0}\hat{q}_2^2}{P_0^4(P_{D_0}+\check{q}_4)^2} =: \hat{\rho}_2, \qquad \text{for } u \in Q_2, \quad v \in Q_4,\\
0 \leqslant \left|\frac{\mathrm{d}g_{\mathrm{D}}(u)}{\mathrm{d}u}\right| &\leqslant \frac{2a_2k_{\mathrm{D}}k_{\mathrm{H}}}{P_0^2 d_1 d_2} =: \hat{\rho}_3, \qquad \text{for } u \in Q_2.
\end{aligned} \tag{2.11}$$

Note that $\hat{\rho}_i$ is computable and $\hat{\rho}_i \geqslant \rho_i$, $i = 1, 2, 3$. Therefore, the convergent result in theorem 2.6 also holds under the following condition

$$\hat{\rho}_1 a_2 d_3 d_4 + \hat{\rho}_2\hat{\rho}_3 a_2 a_4 < \beta_4, \tag{2.12}$$

which is easier to verify from computation view point. (ii) Roughly speaking, condition (2.10) in theorem 2.6 favors large decay rates and small synthesis rates. (iii) Recalling remark 2.1(i), we can establish smaller attracting region $\mathcal{Q}$ if further iterative estimate is performed. Subsequently, the value ρ_i (respectively, $\hat{\rho}_i$) can be lowered to relax condition (2.10) (respectively, (2.12)). (iv) Under condition (2.10) or (2.12), $\bar{\mathbb{X}}$ obtained in proposition 2.3 is the unique positive equilibrium for system (1.1), according to theorem 2.6.

Theorem 2.6 asserts that

$$x_i(t) \to \bar{x}_i \quad \text{and} \quad y_i(t) \to \bar{x}_i, \qquad \text{as } t \to \infty, \quad i = 1, 2, 3, 4,$$

for solution $\mathbb{X}(t) = (x_1(t), \ldots, x_4(t), y_1(t), \ldots, y_4(t))$ of system (1.1), evolved from any initial condition in $\mathcal{C}([-\tau_M, 0], \mathbb{R}_+^8)$. This corresponds to non-oscillatory or oscillation-arrested phase for system (1.1), which is associated with the state of formed somites. This scenario also corresponds to the global synchronization of system (1.1), as

$$x_i(t) - y_i(t) \to \bar{x}_i - \bar{x}_i = 0, \qquad \text{as} \quad t \to \infty, \quad i = 1, 2, 3, 4.$$

In fact, by analyzing the difference system $\frac{\mathrm{d}}{\mathrm{d}t}(x_i(t) - y_i(t))$, and employing arguments similar to those in proposition 2.5, we can establish the global synchronization for system (1.1) directly, also under condition (2.10).

Corollary 2.7. *Under condition (2.10) or (2.12), system (1.1) attains global synchronization:* $x_i(t) - y_i(t) \to 0$, as $t \to \infty$, $i = 1, 2, 3, 4$, *for solution* $(x_1(t), \ldots, x_4(t), y_1(t), \ldots, y_4(t))$ *of system (1.1), evolved from any initial condition in* $\mathcal{C}([-\tau_M, 0], \mathbb{R}_+^8)$.

It is usually a challenging task to investigate global dynamics for nonlinear systems and delay coupled systems. Without knowing and using Lyapunov function, the above iteration formulation works well in deriving global synchronization and global convergence to the synchronous equilibrium.

3. Synchronous oscillations

Although corollary 2.7 concludes the global synchronization, it does reduce to the situation that every solution tends to the synchronous steady state. Thus, there does not exist any oscillation for system (1.1), under condition (2.10) or (2.12). In this section, we turn to target the local dynamics and employ bifurcation theory to investigate the synchronous oscillations.

We shall apply the delay Hopf bifurcation theory to prove the existence of nontrivial synchronous periodic solutions for system (1.1), in section 3.1. We then use the center manifold theorem and the normal form method to compute the stability of the bifurcated

periodic solutions in section 3.2. With positive invariance of the synchronous manifold, the result then leads to synchronous oscillations for (1.1). To depict the loss of synchrony and the phase transition as parameters or delay magnitudes vary, the asynchronous oscillation will also be discussed.

3.1. Bifurcation of periodic orbits

In this section, we shall investigate the periodic solutions bifurcated from the synchronous equilibrium $\bar{\mathbb{X}}$ of system (1.1) via Hopf bifurcation theorem. By observing the structure of the characteristic equation, while holding $s = \tau_3 + \tau_4$ fixed, we take $r = \tau_1 + \tau_2$ as the bifurcation parameter. We will work on system (2.5) which is a translation of (1.1) from $\bar{\mathbb{X}}$ to the origin. The linearization of system (2.5) at the origin is given by

$$\begin{aligned}
\dot{x}_1(t) &= -d_1 x_1(t) + \ell_{11} x_2(t-\tau_1) + \ell_{12} y_4(t-\tau_1),\\
\dot{x}_2(t) &= -d_2 x_2(t) + a_2 x_1(t-\tau_2),\\
\dot{x}_3(t) &= -d_3 x_3(t) + \ell_{31} x_2(t-\tau_3),\\
\dot{x}_4(t) &= -d_4 x_4(t) + a_4 x_3(t-\tau_4),\\
\dot{y}_1(t) &= -d_1 y_1(t) + \ell_{51} y_2(t-\tau_1) + \ell_{52} x_4(t-\tau_1),\\
\dot{y}_2(t) &= -d_2 y_2(t) + a_2 y_1(t-\tau_2),\\
\dot{y}_3(t) &= -d_3 y_3(t) + \ell_{71} y_2(t-\tau_3),\\
\dot{y}_4(t) &= -d_4 y_4(t) + a_4 y_3(t-\tau_4),
\end{aligned} \tag{3.1}$$

where

$$\ell_{11} = \ell_{51} := \frac{\partial g_{\mathrm{H}}}{\partial u}(\bar{x}_2, \bar{x}_4), \quad \ell_{12} = \ell_{52} := \frac{\partial g_{\mathrm{H}}}{\partial v}(\bar{x}_2, \bar{x}_4), \quad \ell_{31} = \ell_{71} := \frac{\mathrm{d} g_{\mathrm{D}}}{\mathrm{d} u}(\bar{x}_2). \tag{3.2}$$

For convenience, we set

$$\begin{aligned}
\gamma_1 &:= -\frac{\partial g_{\mathrm{H}}}{\partial u}(u, v)|_{u=\bar{x}_2, v=\bar{x}_4} = \frac{2k_{\mathrm{H}} P_0^2 P_{D_0} \bar{x}_2 (P_{D_0} + \bar{x}_4)}{[P_{D_0}(P_0^2 + \bar{x}_2^2) + P_0^2 \bar{x}_4]^2},\\
\gamma_2 &:= \frac{\partial g_{\mathrm{H}}}{\partial v}(u, v)|_{u=\bar{x}_2, v=\bar{x}_4} = \frac{k_{\mathrm{H}} P_0^2 P_{D_0} \bar{x}_2^2}{[P_{D_0}(P_0^2 + \bar{x}_2^2) + P_0^2 \bar{x}_4]^2},\\
\gamma_3 &:= -\frac{\mathrm{d} g_{\mathrm{D}}}{\mathrm{d} u}(u)|_{u=\bar{x}_2} = \frac{2k_{\mathrm{D}} P_0^2 \bar{x}_2}{(P_0^2 + \bar{x}_2^2)^2}.
\end{aligned}$$

Indeed, $\gamma_1 = -\ell_{11} = -\ell_{51}$, $\gamma_2 = \ell_{12} = \ell_{52}$, $\gamma_3 = -\ell_{31} = -\ell_{71}$ and $\gamma_1, \gamma_2, \gamma_3 > 0$. The characteristic equation for (3.1) is

$$\Delta(\lambda, \tau_1, \tau_2, \tau_3, \tau_4) = 0, \tag{3.3}$$

where $\Delta(\lambda, \tau_1, \tau_2, \tau_3, \tau_4)$ is given by

$$\det \begin{pmatrix}
\lambda + d_1 & \gamma_1 \mathrm{e}^{-\tau_1 \lambda} & 0 & 0 & 0 & 0 & 0 & -\gamma_2 \mathrm{e}^{-\tau_1 \lambda}\\
-a_2 \mathrm{e}^{-\tau_2 \lambda} & \lambda + d_2 & 0 & 0 & 0 & 0 & 0 & 0\\
0 & \gamma_3 \mathrm{e}^{-\tau_3 \lambda} & \lambda + d_3 & 0 & 0 & 0 & 0 & 0\\
0 & 0 & -a_4 \mathrm{e}^{-\tau_4 \lambda} & \lambda + d_4 & 0 & 0 & 0 & 0\\
0 & 0 & 0 & -\gamma_2 \mathrm{e}^{-\tau_1 \lambda} & \lambda + d_1 & \gamma_1 \mathrm{e}^{-\tau_1 \lambda} & 0 & 0\\
0 & 0 & 0 & 0 & -a_2 \mathrm{e}^{-\tau_2 \lambda} & \lambda + d_2 & 0 & 0\\
0 & 0 & 0 & 0 & 0 & \gamma_3 \mathrm{e}^{-\tau_3 \lambda} & \lambda + d_1 & 0\\
0 & 0 & 0 & 0 & 0 & 0 & -a_4 \mathrm{e}^{-\tau_4 \lambda} & \lambda + d_4
\end{pmatrix}.$$

By letting $r := \tau_1 + \tau_2$ and $s := \tau_3 + \tau_4$, the characteristic equation (3.3) can be factored as

$$\Delta_+(\lambda, \tau_1, \tau_2, \tau_3, \tau_4) \cdot \Delta_-(\lambda, \tau_1, \tau_2, \tau_3, \tau_4) = \Delta_+(\lambda, r, s) \cdot \Delta_-(\lambda, r, s) = 0, \tag{3.4}$$

where

$$\begin{aligned}
\Delta_\pm(\lambda, \tau_1, \tau_2, \tau_3, \tau_4) &:= \lambda^4 + \beta_1\lambda^3 + \beta_2\lambda^2 + \beta_3\lambda + \beta_4 \\
&\quad + a_2\gamma_1[\lambda^2 + (d_3 + d_4)\lambda + d_3d_4]\mathrm{e}^{-(\tau_1+\tau_2)\lambda} \pm a_2a_4\gamma_2\gamma_3\mathrm{e}^{-(\tau_1+\tau_2+\tau_3+\tau_4)\lambda}, \\
\Delta_\pm(\lambda, r, s) &:= \lambda^4 + \beta_1\lambda^3 + \beta_2\lambda^2 + \beta_3\lambda + \beta_4 \\
&\quad + a_2\gamma_1[\lambda^2 + (d_3 + d_4)\lambda + d_3d_4]\mathrm{e}^{-r\lambda} \pm a_2a_4\gamma_2\gamma_3\mathrm{e}^{-(r+s)\lambda}, \\
\beta_1 &:= d_1 + d_2 + d_3 + d_4, \\
\beta_2 &:= d_2d_4 + d_3d_4 + d_2d_3 + d_1d_4 + d_1d_2 + d_1d_3, \\
\beta_3 &:= d_2d_3d_4 + d_1d_2d_4 + d_1d_3d_4 + d_1d_2d_3,
\end{aligned} \tag{3.5}$$

and β_4 has been introduced in (2.10). Note that each β_i is positive.

We now investigate, for fixed $s \geqslant 0$, the existence of r-induced periodic solutions bifurcated from the origin of (2.5). We shall start from finding a purely imaginary root $\mathrm{i}w$ of the characteristic equation (3.3) and its corresponding bifurcation value $r = r(w)$ so that $\Delta(\mathrm{i}w, r(w), s) = 0$. To this end, we substitute $\lambda = \mathrm{i}w$, with $w > 0$, into $\Delta_\pm(\lambda, r, s) = 0$ and collect the real and imaginary parts:

$$\begin{aligned}
&w^4 - \beta_2w^2 + \beta_4 + a_2\gamma_1(d_3d_4 - w^2)\cos(rw) + a_2\gamma_1w(d_3 + d_4)\sin(rw) \\
&\qquad \pm a_2a_4\gamma_2\gamma_3\cos((r + s)w) = 0, \\
&-\beta_1w^3 + \beta_3w + a_2\gamma_1w(d_3 + d_4)\cos(rw) + a_2\gamma_1(w^2 - d_3d_4)\sin(rw) \\
&\qquad \mp a_2a_4\gamma_2\gamma_3\sin((r + s)w) = 0.
\end{aligned} \tag{3.6}$$

By the properties of trigonometric functions, (3.6) can be written as

$$\begin{aligned}
&w^4 - \beta_2w^2 + \beta_4 + [a_2\gamma_1(d_3d_4 - w^2) \pm a_2a_4\gamma_2\gamma_3\cos(sw)]\cos(rw) \\
&\qquad + [a_2\gamma_1w(d_3 + d_4) \mp a_2a_4\gamma_2\gamma_3\sin(sw)]\sin(rw) = 0, \\
&-\beta_1w^3 + \beta_3w + [a_2\gamma_1w(d_3 + d_4) \mp a_2a_4\gamma_2\gamma_3\sin(sw)]\cos(rw) \\
&\qquad - [a_2\gamma_1(d_3d_4 - w^2) \pm a_2a_4\gamma_2\gamma_3\cos(sw)]\sin(rw) = 0,
\end{aligned}$$

or, equivalently,

$$\begin{aligned}
\sqrt{L_\pm(w)} \cdot \sin(\phi_\pm + rw) &= -w^4 + \beta_2w^2 - \beta_4, \\
\sqrt{L_\pm(w)} \cdot \cos(\phi_\pm + rw) &= \beta_1w^3 - \beta_3w,
\end{aligned} \tag{3.7}$$

where $L_\pm(w) := [a_2\gamma_1(d_3d_4 - w^2) \pm a_2a_4\gamma_2\gamma_3\cos(sw)]^2 + [a_2\gamma_1w(d_3 + d_4) \mp a_2a_4\gamma_2\gamma_3\sin(sw)]^2 > 0$, if w is a solution of (3.7); $\phi_\pm \in [0, 2\pi)$ and satisfies

$$\begin{aligned}
\sin(\phi_\pm) &= [a_2\gamma_1(d_3d_4 - w^2) \pm a_2a_4\gamma_2\gamma_3\cos(sw)]/\sqrt{L_\pm(w)}, \\
\cos(\phi_\pm) &= [a_2\gamma_1w(d_3 + d_4) \mp a_2a_4\gamma_2\gamma_3\sin(sw)]/\sqrt{L_\pm(w)}.
\end{aligned}$$

Summing up the square of equations (3.7) gives

$$Q_\pm(w) = (a_2d_3d_4\gamma_1)^2 =: \Gamma, \tag{3.8}$$

where

$$\begin{aligned}
Q_\pm(w) &= w^8 + (\beta_1^2 - 2\beta_2)w^6 + (-a_2^2\gamma_1^2 + \beta_2^2 - 2\beta_1\beta_3 + 2\beta_4)w^4 \\
&\quad + [-a_2^2(d_3^2 + d_4^2)\gamma_1^2 + \beta_3^2 - 2\beta_2\beta_4 \pm 2a_2^2a_4\gamma_1\gamma_2\gamma_3\cos(sw)]w^2 \\
&\quad \pm [2a_2^2a_4(d_3 + d_4)\gamma_1\gamma_2\gamma_3\sin(sw)]w \\
&\quad + [\beta_4^2 - a_2^2a_4^2\gamma_2^2\gamma_3^2 \mp 2a_2^2a_4d_3d_4\gamma_1\gamma_2\gamma_3\cos(sw)].
\end{aligned}$$

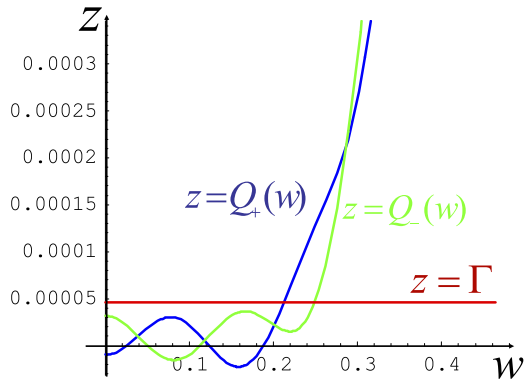

Figure 1. Graphs of functions $z = Q_-(w)$, $z = Q_+(w)$, $z = \Gamma$, with the parameter data in [25].

We summarize the properties of functions $Q_\pm(w)$ as follows; cf figure 1.

(P1) : $Q_\pm(0) = \beta_4^2 - (a_2a_4\gamma_2\gamma_3)^2 \mp 2a_2^2a_4d_3d_4\gamma_1\gamma_2\gamma_3$. Obviously,
$$Q_+(0) < Q_-(0).$$

(P2) : $Q_+(w)$ and $Q_-(w)$ are dominated by the leading term w^8, since $|\sin u|, |\cos u| \leqslant 1$. Consequently, both $Q_+(w)$ and $Q_-(w)$ are strictly increasing eventually, and increase to ∞, as $w \to \infty$.

According to properties (P1) and (P2), we derive the following lemma.

Lemma 3.1.

(i) For any fixed $s \geqslant 0$, there exists at least a positive solution to $Q_+(w) = \Gamma$ if $Q_+(0) < \Gamma$; namely,
$$0 < \beta_4 < a_2a_4\gamma_2\gamma_3 + a_2d_3d_4\gamma_1. \tag{3.9}$$

(ii) For any fixed $s \geqslant 0$, each of $Q_-(w) = \Gamma$ and $Q_+(w) = \Gamma$ has at least a positive solution if $Q_-(0) < \Gamma$; namely,
$$0 < \beta_4 < |a_2a_4\gamma_2\gamma_3 - a_2d_3d_4\gamma_1|. \tag{3.10}$$

There may exist multiple solutions to $Q_+(w) = \Gamma$ or $Q_-(w) = \Gamma$. In the following, we denote by w_+ (respectively, w_-) a positive solution to $Q_+(\cdot) = \Gamma$ (respectively, $Q_-(\cdot) = \Gamma$). Now, we find the value of r such that $\mathrm{i}w_\pm$ is a purely imaginary root of $\Delta_\pm(\cdot, r, s) = 0$. We divide the first equation of (3.7) by the second and obtain
$$\tan(\phi_\pm + rw) = S(w)/C(w),$$
$$S(w) := -w^4 + \beta_2w^2 - \beta_4,$$
$$C(w) := \beta_1w^3 - \beta_3w.$$
Let $\sigma = +$ or $-$. For a fixed w_σ, there exists a sequence $\{r_\sigma^{(k)}(w_\sigma)\}_{k\in\mathbb{Z}}$:
$$r_\sigma^{(k)}(w_\sigma) := \begin{cases} \dfrac{1}{w_\sigma}\left[\tan^{-1}\left(\dfrac{S(w_\sigma)}{C(w_\sigma)}\right) - \phi_\sigma + 2k\pi\right], & \text{if } C(w_\sigma) > 0\,, \\ \dfrac{1}{w_\sigma}\left[\tan^{-1}\left(\dfrac{S(w_\sigma)}{C(w_\sigma)}\right) - \phi_\sigma + (2k-1)\pi\right], & \text{if } C(w_\sigma) < 0\,, \\ \dfrac{1}{w_\sigma}\left[\dfrac{3\pi}{2} - \phi_\sigma + 2k\pi\right], & \text{if } C(w_\sigma) = 0,\ S(w_\sigma) < 0, \\ \dfrac{1}{w_\sigma}\left[\dfrac{\pi}{2} - \phi_\sigma + 2k\pi\right], & \text{if } C(w_\sigma) = 0,\ S(w_\sigma) > 0, \end{cases} \tag{3.11}$$

such that $\Delta_\sigma(\mathrm{i}w_\sigma, r_\sigma^{(k)}(w_\sigma), s) = 0$. To simplify the notation, we denote $r_\sigma^{(k)} := r_\sigma^{(k)}(w_\sigma)$ as the bifurcation value, and we shall consider the case $r_\sigma^{(k)} > 0$. Accordingly, a positive solution w_+ (respectively, w_-) of $Q_+(\cdot) = \Gamma$ (respectively, $Q_-(\cdot) = \Gamma$) corresponds to a pair of purely imaginary roots $\pm\mathrm{i}w_+$ (respectively, $\pm\mathrm{i}w_-$) of $\Delta_+(\cdot, r_+^{(k)}, s) = 0$ (respectively, $\Delta_-(\cdot, r_-^{(k)}, s) = 0$).

Next, to apply Hopf bifurcation theory, we further impose the conditions of simple root and transversality. For $\sigma = +, -$, we consider

Condition $(\mathrm{C1})_\sigma$: $Q'_\sigma(w_\sigma) \neq 0$, and all other positive solutions to $Q_+(\cdot) = \Gamma$ and $Q_-(\cdot) = \Gamma$ are not integer multiples of w_σ.

Condition $(\mathrm{C2})_\sigma$: $[R_\sigma(w_\sigma, r_\sigma^{(k)})]^2 + [I_\sigma(w_\sigma, r_\sigma^{(k)})]^2 \neq 0$, $W_{1,\sigma}^2(w_\sigma, r_\sigma^{(k)}) + W_{2,\sigma}^2(w_\sigma, r_\sigma^{(k)}) \neq 0$, and $Q_{1,\sigma}(w_\sigma, r_\sigma^{(k)})W_{1,\sigma}(w_\sigma, r_\sigma^{(k)}) + Q_{2,\sigma}(w_\sigma, r_\sigma^{(k)})W_{2,\sigma}(w_\sigma, r_\sigma^{(k)}) \neq 0$, where

$$\begin{aligned}
R_\pm(w, r) &:= -3w^2\beta_1 + \beta_3 + a_2\gamma_1(d_3 + d_4 - d_3d_4r + w^2r)\cos(wr)\\
&\quad -a_2\gamma_1 w(-2 + d_3r + d_4r)\sin(wr) \mp a_2a_4\gamma_2\gamma_3(r + s)\cos((r + s)w),\\
I_\pm(w, r) &:= -4w^3 + 2w\beta_2 - a_2\gamma_1 w(-2 + d_3r + d_4r)\cos(wr)\\
&\quad -a_2\gamma_1(d_3 + d_4 - d_3d_4r + w^2r)\sin(wr) \pm a_2a_4\gamma_2\gamma_3(r + s)\sin((r + s)w),\\
Q_{1,\pm}(w, r) &:= -a_2w[(d_3 + d_4)\gamma_1 w\cos(wr) + \gamma_1(-d_3d_4 + w^2)\sin(wr)\\
&\quad \mp a_4\gamma_2\gamma_3\sin((r + s)w)],\\
Q_{2,\pm}(w, r) &:= a_2w[\gamma_1(d_3d_4 - w^2)\cos(wr) \pm a_4\gamma_2\gamma_3\cos((r + s)w)\\
&\quad +(d_3 + d_4)\gamma_1 w\sin(wr)],\\
W_{1,\pm}(w, r) &:= -3w^2\beta_1 + \beta_3 + a_2\gamma_1(d_3 + d_4 - d_3d_4r + w^2r)\cos(wr)\\
&\quad \mp a_2a_4\gamma_2\gamma_3(r + s)\cos((r + s)w) - a_2\gamma_1 w(-2 + d_3r + d_4r)\sin(wr),\\
W_{2,\pm}(w, r) &:= -[4w^3 - 2w\beta_2 + a_2\gamma_1 w(-2 + d_3r + d_4r)\cos(wr)\\
&\quad +a_2\gamma_1(d_3 + d_4 - d_3d_4r + w^2r)\sin(wr) \mp a_2a_4\gamma_2\gamma_3(r + s)\sin((r + s)w)].
\end{aligned}$$

These terms are obtained from the proof of the following theorem.

Theorem 3.2. *For a fixed $s \geqslant 0$, assume that there exists a positive solution w_+ (respectively, w_-) to $Q_+(w) = \Gamma$ (respectively, $Q_-(w) = \Gamma$) satisfying conditions $(C1)_+$ and $(C2)_+$ (respectively, $(C1)_-$ and $(C2)_-$) for some $r_+^{(k)} > 0$ (respectively, $r_-^{(k)} > 0$) and $k \in \mathbb{Z}$. Then Hopf bifurcation occurs at $r = r_+^{(k)}$ (respectively, $r = r_-^{(k)}$), and a periodic orbit is bifurcated from the zero solution of system (2.5). Moreover, the periodic orbit bifurcated at $r_+^{(k)} > 0$ is synchronous, while the one bifurcated at $r_-^{(k)} > 0$ is asynchronous.*

Proof. Under the assumption, it suffices to verify the transversality for the assertion of Hopf bifurcation. We only prove the first case. We compute that

$$\begin{aligned}
\frac{\partial}{\partial\lambda}\Delta_+(\lambda, r, s)|_{\lambda=\mathrm{i}w_+, r=r_+^{(k)}} &= \{4\lambda^3 + 3\beta_1\lambda^2 + 2\beta_2\lambda + \beta_3 + a_2\gamma_1(2\lambda + d_3 + d_4)\mathrm{e}^{-r\lambda}\\
&\quad -ra_2\gamma_1[\lambda^2 + (d_3 + d_4)\lambda + d_3d_4]\mathrm{e}^{-r\lambda} - (r + s)a_2a_4\gamma_2\gamma_3\mathrm{e}^{-(r+s)\lambda}\}|_{\lambda=\mathrm{i}w_+, r=r_+^{(k)}}\\
&= R_+(w_+, r_+^{(k)}) + \mathrm{i}I_+(w_+, r_+^{(k)}),
\end{aligned}$$

where R_+, I_+ are defined as above. Thus, $\frac{\partial}{\partial\lambda}\Delta_+(\lambda, r, s)|_{\lambda=\mathrm{i}w_+, r=r_+^{(k)}} \neq 0$, due to condition $(\mathrm{C2})_+$. Hence, there exist a $\delta_+^{(k)} > 0$ and a smooth function $\lambda_+^{(k)} : (r_+^{(k)} - \delta_+^{(k)}, r_+^{(k)} + \delta_+^{(k)}) \to \mathbb{C}$ such that $\Delta_+(\lambda_+^{(k)}(r_+^{(k)}), r_+^{(k)}, s) = \Delta_+(\lambda_+^{(k)}(r_+^{(k)})) = 0$ and $\lambda_+^{(k)}(r_+^{(k)}) = \mathrm{i}w_+$, by the implicit function theorem. Differentiating $\Delta_+(\lambda_+^{(k)}(r)) = 0$ with respect to r at $r = r_+^{(k)}$, we obtain

$$(\lambda_+^{(k)})'(r_+^{(k)}) = \frac{Q_{1,+}(w_+, r_+^{(k)}) + \mathrm{i}Q_{2,+}(w_+, r_+^{(k)})}{W_{1,+}(w_+, r_+^{(k)}) + \mathrm{i}W_{2,+}(w_+, r_+^{(k)})},$$

where $Q_{1,+}$, $Q_{2,+}$, $W_{1,+}$, $W_{2,+}$ are defined as above. Thus, $\mathrm{Re}((\lambda_+^{(k)})'(r_+^{(k)})) \neq 0$, by condition $(C2)_+$. Therefore, Hopf bifurcation occurs at the origin of system (2.5) at $r = r_+^{(k)}$, according to [15]. Next, note that

$$\mathcal{S} := \{(z_1, z_2, z_3, z_4, z_1, z_2, z_3, z_4) : z_i \in \mathcal{C}([-\tau_M, 0], \mathbb{R}_+), i = 1, 2, 3, 4\} \tag{3.12}$$

is positively invariant under (1.1) and (2.5). In addition, the characteristic equation for the linearized system of (2.5) restricted to the synchronous manifold $\mathcal{S}$ at the origin, is exactly $\Delta_+(\lambda, r, s) = 0$. Therefore, by the uniqueness in Hopf bifurcation theorem and the positive invariance of $\mathcal{S}$, the periodic orbit generated by the bifurcation at $r = r_+^{(k)}$ is synchronous. On the other hand, the periodic orbit generated by the bifurcation at $r = r_-^{(k)}$ is asynchronous; cf [14, 20, 39] for details. □

Remark 3.1. (i) In lemma 3.1, (3.9) and (3.10) are sufficient conditions for $Q_+(w) = \Gamma$ and $Q_\pm(w) = \Gamma$ to have a solution, respectively. These conditions provide a basic parameter range for $\Delta_\pm(\cdot, r, s) = 0$ to admit purely imaginary roots. Therefore, theorem 3.2 can be used with condition (3.9) or (3.10). For parameters not satisfying (3.9) or (3.10), we still can compute all positive solutions to $Q_\pm(w) = \Gamma$ numerically, if they exist. (ii) It is also possible to use s as the bifurcation parameter, as observed from the structure of the characteristic equation for (3.1). The computation will be similar to using r. (iii) We have seen that β_4, the product of all decay rates d_i, $i = 1, 2, 3, 4$, has appeared in the conditions for theorem 2.6 and lemma 3.1. The parameters corresponding to the stable synchronous oscillations lie outside the range for global convergence to the equilibrium in theorem 2.6, namely,

$$\beta_4 \leqslant \rho_1 a_2 d_3 d_4 + \rho_2 \rho_3 a_2 a_4.$$

Indeed, β_4 serves as an organizer for the dynamics of system (1.1). We shall pursue this further in the next section.

3.2. Stability of periodic solution

Under the situation that there exist solutions w_+ to $Q_+(\cdot) = \Gamma$ and/or w_- to $Q_-(\cdot) = \Gamma$, the following value r_c which stands for the first bifurcation value of r can be defined:

$$\begin{aligned} r_c := \ & \min\{r : r = r_+^{(k)}(w_+) > 0 \text{ or } r = r_-^{(k)}(w_-) > 0,\ k \in \mathbb{Z}, \\ & Q_+(w_+) = \Gamma,\ Q_-(w_-) = \Gamma\}. \end{aligned} \tag{3.13}$$

Moreover, we set w_c as the positive solution to $Q_+(\cdot) = \Gamma$ with $r_c = r_+^{(k)}(w_c)$ or to $Q_-(\cdot) = \Gamma$ with $r_c = r_-^{(k)}(w_c)$, for some $k \in \mathbb{Z}$. We note that r_c and w_c are well defined under (3.9) or (3.10).

In this subsection, we shall analyze the stability of the periodic solution induced by $r = \tau_1 + \tau_2$ for system (2.5) at r near r_c, by the normal form theory. To this end, we will first discuss the stability for the equilibrium of the system as $r < r_c$. It will be shown that in some parameter range, the origin of system (2.5) is asymptotically stable for $r < r_c$ and any $\tau_3 \geqslant 0$ and $\tau_4 \geqslant 0$.

We consider (3.4) with $r = 0$; namely,

$$\Delta_+(\lambda, 0, s) \cdot \Delta_-(\lambda, 0, s) = 0. \tag{3.14}$$

We aim at deriving the conditions for parameters under which all roots of (3.14) have negative real parts, for all $s \geqslant 0$. We first consider (3.14) with $s = 0$ as follows:

$$\begin{aligned} &\Delta_+(\lambda, 0, 0) \cdot \Delta_-(\lambda, 0, 0) = 0, \\ &\Delta_\pm(\lambda, 0, 0) = \lambda^4 + \alpha_1\lambda^3 + \alpha_2\lambda^2 + \alpha_3\lambda + \alpha_4^\pm, \end{aligned} \tag{3.15}$$

where $\alpha_1 := \beta_1, \alpha_2 := \beta_2 + a_2\gamma_1, \alpha_3 := \beta_3 + a_2\gamma_1(d_3 + d_4)$ and $\alpha_4^\pm := \beta_4 + a_2d_3d_4\gamma_1 \pm a_2a_4\gamma_2\gamma_3$. For later use, we denote

$$\begin{aligned} D_1 &:= \det(\alpha_1) = \alpha_1 > 0, \\ D_2 &:= \det\begin{pmatrix} \alpha_1 & \alpha_3 \\ 1 & \alpha_2 \end{pmatrix} \\ &= d_4^2(d_1 + d_2 + d_3) + d_4(d_1 + d_2 + d_3)^2 + (d_1 + d_2)[d_3^2 + d_1d_3 + d_2(d_1 + d_3) + a_2\gamma_1] > 0, \\ D_3^\pm &:= \det\begin{pmatrix} \alpha_1 & \alpha_3 & 0 \\ 1 & \alpha_2 & \alpha_4^\pm \\ 0 & \alpha_1 & \alpha_3 \end{pmatrix} = \alpha_1\alpha_2\alpha_3 - \alpha_3^2 - \alpha_1^2\alpha_4^\pm, \\ D_4^\pm &:= \det\begin{pmatrix} \alpha_1 & \alpha_3 & 0 & 0 \\ 1 & \alpha_2 & \alpha_4^\pm & 0 \\ 0 & \alpha_1 & \alpha_3 & 0 \\ 0 & 1 & \alpha_2 & \alpha_4^\pm \end{pmatrix} = \alpha_4^\pm \cdot D_3^\pm. \end{aligned}$$

Note that D_1 and D_2 are both positive. Therefore, by the well-known Routh–Hurwitz criterion, all roots of (3.15) have negative real parts if and only if

$$D_3^+ > 0, \qquad D_3^- > 0, \qquad D_4^+ > 0 \qquad \text{and} \qquad D_4^- > 0. \tag{3.16}$$

Now, we give the following result on the stability of the origin for (2.5) with $r = s = 0$.

Lemma 3.3. *All roots of (3.15) have negative real parts, and hence the origin of system (2.5) with $r = s = 0$ is asymptotically stable if and only if*

$$\frac{\alpha_1\alpha_2\alpha_3 - (\alpha_3)^2}{(\alpha_1)^2} - a_2a_4\gamma_2\gamma_3 - a_2d_3d_4\gamma_1 > \beta_4 > a_2a_4\gamma_2\gamma_3 - a_2d_3d_4\gamma_1. \tag{3.17}$$

Proof. Note that $\alpha_4^+ > \alpha_4^-$ and $D_3^+ < D_3^-$. Thus $\alpha_4^- > 0$ and $D_3^+ > 0$ if and only if (3.16) holds. It can be verified that (3.17) holds if and only if $\alpha_4^- > 0$ and $D_3^+ > 0$. The assertion thus follows. □

Following lemma 3.3, we shall show that the origin is an asymptotically stable equilibrium of (2.5), for any $s \geqslant 0$ and $r = 0$ under some additional condition. We substitute $\lambda = \mathrm{i}\nu$ with $\nu \geqslant 0$ into $\Delta_\pm(\lambda, 0, s) = 0$ and collect the real and imaginary parts to obtain

$$\begin{aligned} &\mp a_2a_4\gamma_2\gamma_3 \cos(\nu s) = \nu^4 + a_2\gamma_1(d_3d_4 - \nu^2) - \beta_2\nu^2 + \beta_4, \\ &\pm a_2a_4\gamma_2\gamma_3 \sin(\nu s) = \nu[a_2(d_3 + d_4)\gamma_1 - \nu^2\beta_1 + \beta_3]. \end{aligned} \tag{3.18}$$

Summing up the square of equations (3.18) gives

$$E(\nu) = (a_2a_4\gamma_2\gamma_3)^2, \tag{3.19}$$

where

$$E(\nu) = \nu^8 + (-2a_2\gamma_1 + \beta_1^2 - 2\beta_2)\nu^6 + [a_2^2\gamma_1^2 + \beta_2^2 + 2a_2\gamma_1(d_3d_4 - (d_3 + d_4)\beta_1 + \beta_2) - 2\beta_1\beta_3 + 2\beta_4]\nu^4 + [a_2^2(d_3^2 + d_4^2)\gamma_1^2 + \beta_3^2 - 2\beta_2\beta_4 - 2a_2\gamma_1(d_3d_4\beta_2 - (d_3 + d_4)\beta_3 + \beta_4)]\nu^2 + (a_2d_3d_4\gamma_1 + \beta_4)^2.$$

A direct computation gives $E'(\nu) = 8\nu^7 + E_5\nu^5 + E_3\nu^3 + E_1\nu$, where

$$E_5 = 6(d_1^2 + d_2^2 + d_3^2 + d_4^2) - 12a_2\gamma_1,$$
$$E_3 = 4[d_1^2d_3^2 + d_2^2(d_1^2 + d_3^2) + 2a_2d_1d_2\gamma_1 + a_2^2\gamma_1^2 + d_4^2(d_1^2 + d_2^2 + d_3^2)] - 8a_2(d_3^2 + d_4^2)\gamma_1,$$
$$E_1 = 2[d_3^2(d_1d_2 + a_2\gamma_1)^2 + d_4^2(d_2^2(d_1^2 + d_3^2) + 2a_2d_1d_2\gamma_1 + a_2^2\gamma_1^2 + d_1^2d_3^2)] - 4d_3^2d_4^2a_2\gamma_1.$$

Lemma 3.4. *There does not exist any real solution to (3.19) under conditions:*

$$E_1 > 0, \qquad E_3 > 0, \qquad E_5 > 0, \tag{3.20}$$
$$\beta_4 > a_2a_4\gamma_2\gamma_3 - a_2d_3d_4\gamma_1. \tag{3.21}$$

Proof. Obviously, $E(\nu)$ is strictly increasing on $[0, \infty)$, under condition (3.20). Moreover, it is straightforward to verify that $E(0) = (a_2d_3d_4\gamma_1 + \beta_4)^2 > (a_2a_4\gamma_2\gamma_3)^2$ if (3.21) holds. Consequently, $E(\nu) > (a_2a_4\gamma_2\gamma_3)^2$, for all $\nu \geqslant 0$, and hence for all $\nu \in \mathbb{R}$, as E is an even function. □

Remark 3.2. By the definition of E_i and that γ_1 is bounded, we find that, roughly speaking, inequalities (3.20) favor larger d_1 and d_2 and smaller a_2, d_3 and d_4. Note that (3.17) implies (3.21).

By lemmas 3.3 and 3.4, for arbitrarily fixed $s \geqslant 0$ and $r = 0$, all roots of (3.14) have negative real parts under conditions (3.17) and (3.20). Moreover, under such assumptions, there does not exist any solution λ with nonnegative real part to $\Delta_\pm(\lambda, r, s) = 0$ for $r < r_c$ and any $s \geqslant 0$. Accordingly, we conclude the following result.

Proposition 3.5. *Assume that (3.9) or (3.10) holds. For any fixed $s \geqslant 0$, the origin is an asymptotically stable equilibrium of system (2.5) for $r < r_c$, under (3.17) and (3.20).*

Remark 3.3. (i) In lemma 3.1, condition (3.9) or (3.10) is used to guarantee the existence of purely imaginary roots $iw_\pm$ for $\Delta_\pm(\cdot, r, s) = 0$. Herein, condition (3.10) is compatible with (3.21) as $a_2a_4\gamma_2\gamma_3 - a_2d_3d_4\gamma_1 < 0$. If $a_2a_4\gamma_2\gamma_3 - a_2d_3d_4\gamma_1 > 0$, we still can use (3.9) to find the solution of $Q_+(w) = \Gamma$, when β_4 satisfies (3.21). (ii) If both $Q_+(w) = \Gamma$ and $Q_-(w) = \Gamma$ do not have any solution, then for any fixed $s \geqslant 0$ and $r \geqslant 0$, the origin is an asymptotically stable equilibrium of system (2.5), under (3.17) and (3.20).

Setting $\sigma = +$ (respectively, $\sigma = -$) if $Q_+(w_c) = \Gamma$ (respectively, $Q_-(w_c) = \Gamma$), we introduce the following conditions:

Condition (B1): $Q_\sigma'(w_c) \neq 0$, and all other positive solutions to $Q_+(\cdot) = \Gamma$ and $Q_-(\cdot) = \Gamma$ satisfy $w \neq mw_c$ for any integer m;
Condition (B2): $[R_\sigma(w_c, r_c)]^2 + [I_\sigma(w_c, r_c)]^2 \neq 0$, $W_{1,\sigma}^2(w_c, r_c) + W_{2,\sigma}^2(w_c, r_c) \neq 0$, and $Q_{1,\sigma}(w_c, r_c)W_{1,\sigma}(w_c, r_c) + Q_{2,\sigma}(w_c, r_c)W_{2,\sigma}(w_c, r_c) \neq 0$.

Conditions (B1), (B2) are analogous to $(C1)_\sigma$, $(C2)_\sigma$, but are specifically considered at w_c and r_c. Moreover, under conditions (B1) and (B2), Hopf bifurcation occurs at the first bifurcation value r_c. Therefore, we shall apply the center manifold theorem and the normal form method to analyze the stability of the periodic solution bifurcated from the origin of system (2.5) and $r = r_c$; cf [15]. Recall that the phase space $\mathcal{C} := \mathcal{C}([-\tau_M, 0], \mathbb{R}^8)$ is a Banach space of continuous functions with the supremum norm $\|\phi\| = \sup_{-\tau_M \leqslant \theta \leqslant 0} |\phi(\theta)|$. We rewrite (2.5) in the following form,

$$\dot{\mathbb{X}}(t) = L_\mu(\mathbb{X}_t) + G_\mu(\mathbb{X}_t), \tag{3.22}$$

where $\mathbb{X}(t) = (x_1(t), \ldots, x_4(t), y_1(t), \ldots, y_4(t))^{\mathrm{T}}$, $\mathbb{X}_t(\theta) = \mathbb{X}(t+\theta)$, $\theta \in [-\tau_M, 0]$, $\mu := r - r_c = \tau_1 + \tau_2 - r_c$, and T denotes the transpose.

The operator $L_\mu : \mathcal{C} \to \mathbb{R}^8$ is the linear part of (3.22), and is given by

$$L_\mu\phi = M_0\phi(0) + M_1\phi(-\tau_1) + M_2\phi(-\tau_2) + M_3\phi(-\tau_3) + M_4\phi(-\tau_4),$$

where $M_0 = \mathrm{diag}\{-d_1, -d_2, -d_3, -d_4, -d_1, -d_2, -d_3, -d_4\}$,

$$(M_1)_{ij} = \begin{cases} \ell_{11}, & \text{if } ij = 12 \\ \ell_{12}, & \text{if } ij = 18 \\ \ell_{52}, & \text{if } ij = 54 \\ \ell_{51}, & \text{if } ij = 56 \\ 0, & \text{otherwise,} \end{cases} \qquad (M_3)_{ij} = \begin{cases} \ell_{31}, & \text{if } ij = 32, \\ \ell_{71}, & \text{if } ij = 76, \\ 0, & \text{otherwise,} \end{cases}$$

$$(M_2)_{ij} = \begin{cases} a_2, & \text{if } ij = 21 \text{ and } ij = 65 \\ 0, & \text{otherwise,} \end{cases} \qquad (M_4)_{ij} = \begin{cases} a_4, & \text{if } ij = 43 \text{ and } ij = 87, \\ 0, & \text{otherwise,} \end{cases}$$

as expressed in (3.1) with $\ell_{11}, \ell_{12}, \ell_{31}, \ell_{51}, \ell_{52}, \ell_{71}$ defined by (3.2). By the Riesz representation theorem, there exists a matrix $\eta(\cdot, \mu)$ whose entries are functions of bounded variation on $[-\tau_M, 0]$ such that $L_\mu\phi = \int_{-\tau_M}^{0} \mathrm{d}\eta(\theta, \mu)\phi(\theta)$. In fact, we can choose

$$\eta(\theta, \mu) = M_0\delta(\theta) + M_1\delta(\theta + \tau_1) + M_2\delta(\theta + \tau_2) + M_3\delta(\theta + \tau_3) + M_4\delta(\theta + \tau_4),$$

where $\delta(\cdot)$ is the Dirac function.

The operator $G_\mu : \mathcal{C} \to \mathbb{R}^8$, is the nonlinear part of (3.22), and is given by

$$G_\mu(\phi) = \begin{pmatrix} m_{11}\phi_2^2(-\tau_1) + m_{12}\phi_2(-\tau_1)\phi_8(-\tau_1) + m_{13}\phi_8^2(-\tau_1) + m_{14}\phi_2^3(-\tau_1) \\ +m_{15}\phi_2^2(-\tau_1)\phi_8(-\tau_1) + m_{16}\phi_2(-\tau_1)\phi_8^2(-\tau_1) + m_{17}\phi_8^3(-\tau_1) + \text{h.o.t.} \\ 0 \\ m_{31}\phi_2^2(-\tau_3) + m_{32}\phi_2^3(-\tau_3) + \text{h.o.t.} \\ 0 \\ m_{51}\phi_6^2(-\tau_1) + m_{52}\phi_6(-\tau_1)\phi_4(-\tau_1) + m_{53}\phi_4^2(-\tau_1) + m_{54}\phi_6^3(-\tau_1) \\ +m_{55}\phi_6^2(-\tau_1)\phi_4(-\tau_1) + m_{56}\phi_6(-\tau_1)\phi_4^2(-\tau_1) + m_{57}\phi_4^3(-\tau_1) + \text{h.o.t.} \\ 0 \\ m_{71}\phi_6^2(-\tau_3) + m_{72}\phi_6^3(-\tau_3) + \text{h.o.t.} \\ 0 \end{pmatrix}, \tag{3.23}$$

where

$$m_{11} = m_{51} := \frac{1}{2}\frac{\partial^2 g_{\mathrm{H}}}{\partial u^2}(\bar{x}_2, \bar{x}_4), \quad m_{12} = m_{52} := \frac{\partial^2 g_{\mathrm{H}}}{\partial u \partial v}(\bar{x}_2, \bar{x}_4),$$

$$m_{13} = m_{53} := \frac{1}{2}\frac{\partial^2 g_{\mathrm{H}}}{\partial v^2}(\bar{x}_2, \bar{x}_4), \quad m_{14} = m_{54} := \frac{1}{6}\frac{\partial^3 g_{\mathrm{H}}}{\partial u^3}(\bar{x}_2, \bar{x}_4),$$

$$m_{15} = m_{55} := \frac{1}{2}\frac{\partial^3 g_{\mathrm{H}}}{\partial u^2 \partial v}(\bar{x}_2, \bar{x}_4), \quad m_{16} = m_{56} := \frac{1}{2}\frac{\partial^3 g_{\mathrm{H}}}{\partial u \partial v^2}(\bar{x}_2, \bar{x}_4),$$

$$m_{17} = m_{57} := \frac{1}{6}\frac{\partial^3 g_{\mathrm{H}}}{\partial v^3}(\bar{x}_2, \bar{x}_4), \quad m_{31} = m_{71} := \frac{1}{2}\frac{\mathrm{d}^2 g_{\mathrm{D}}}{\mathrm{d}u^2}(\bar{x}_2), \quad m_{32} = m_{72} := \frac{1}{6}\frac{\mathrm{d}^3 g_{\mathrm{D}}}{\mathrm{d}u^3}(\bar{x}_2).$$

Now, we define two operators on $\mathcal{C}^1 := \mathcal{C}^1([-\tau_M, 0], \mathbb{R}^8)$:

$$(A_\mu\phi)(\theta) = \begin{cases} \mathrm{d}\phi(\theta)/\mathrm{d}\theta, & \theta \in [-\tau_M,\ 0), \\ \displaystyle\int_{-\tau_M}^{0} \mathrm{d}\eta(\zeta, \mu)\phi(\zeta), & \theta = 0, \end{cases} \tag{3.24}$$

$$(R_\mu\phi)(\theta) = \begin{cases} 0, & \theta \in [-\tau_M,\ 0), \\ G_\mu(\phi), & \theta = 0. \end{cases} \tag{3.25}$$

To analyze the stability of the bifurcated periodic solution by the Hopf bifurcation theory, we transform (3.22) into

$$\dot{\mathbb{X}}_t = A_\mu\mathbb{X}_t + R_\mu\mathbb{X}_t. \tag{3.26}$$

The adjoint operator A^* of A is defined as

$$(A^*_\mu\psi)(\theta^*) = \begin{cases} -\mathrm{d}\psi(\theta^*)/\mathrm{d}\theta^*, & \theta^* \in (0,\ \tau_M], \\ \displaystyle\int_{-\tau_M}^{0} \mathrm{d}\eta^{\mathrm{T}}(\zeta, \mu)\psi(-\zeta), & \theta^* = 0, \end{cases}$$

where $\psi \in \mathcal{C}^1([0, \tau_M], \mathbb{R}^8)$. For convenience, we allow functions to have range in $\mathbb{C}^8$, instead of merely $\mathbb{R}^8$, in the following computation.

To determine the coordinates of the center manifold near the origin of (3.22), we need to use the following bilinear form:

$$\langle\psi, \phi\rangle = \overline{\psi}^{\mathrm{T}}(0)\phi(0) - \int_{\theta=-\tau_M}^{0}\int_{\xi=0}^{\theta} \overline{\psi}^{\mathrm{T}}(\xi - \theta)\,\mathrm{d}\eta(\theta)\phi(\xi)\,\mathrm{d}\xi,$$

for $\phi \in \mathcal{C}([-\tau_M, 0], \mathbb{C}^8)$, $\psi \in \mathcal{C}([0, \tau_M], \mathbb{C}^8)$, where $\eta(\theta) := \eta(\theta, 0)$. Herein, the overline stands for complex conjugate.

Let $q(\theta)$ be the eigenvector of $A := A_0$ corresponding to the purely imaginary eigenvalue $\mathrm{i}w_c$. It follows that $-\mathrm{i}w_c$ is an eigenvalue of $A^* := A_0^*$ with respect to some eigenvector $q^*(\theta^*)$, namely,

$$Aq(\theta) = \mathrm{i}w_c q(\theta) \qquad \text{and} \qquad A^*q^*(\theta^*) = -\mathrm{i}w_c q^*(\theta^*). \tag{3.27}$$

Now, let us compute the eigenvectors $q = q(\theta)$ and $q^* = q^*(\theta^*)$ which satisfy the normalized condition, $\langle q^*, q\rangle = 1$ and $\langle q^*, \bar{q}\rangle = 0$. For this purpose, we assume that

$$q(\theta) = q(0)\mathrm{e}^{\mathrm{i}w_c\theta}, \qquad q^*(\theta^*) = q^*(0)\mathrm{e}^{\mathrm{i}w_c\theta^*}, \tag{3.28}$$

for $\theta \in [-\tau_M, 0]$, $\theta^* \in [0, \tau_M]$, and $q(0) = (q_1, \ldots, q_8)^{\mathrm{T}}$, $q^*(0) = \frac{1}{\rho}(q_1^*, \ldots, q_8^*)^{\mathrm{T}}$, where ρ, q_i and q_i^*, $i = 1, \ldots, 8$, are to be determined. Substituting (3.28) into (3.27) and evaluating at $\theta = 0$, we obtain

$$q_1 = 1, \quad q_2 = \frac{a_2U_2}{V_2}, \quad q_3 = \frac{a_2\ell_{31}U_2U_3}{V_2V_3}, \quad q_4 = \frac{a_2a_4\ell_{31}U_2U_3U_4}{V_2V_3V_4},$$

$$q_5 = \frac{\overline{U}_3\overline{U}_4V_3V_4(-a_2\ell_{11} + \overline{U}_1\overline{U}_2V_1V_2)}{a_2a_4\ell_{12}\ell_{71}}, \quad q_6 = -\frac{\overline{U}_3\overline{U}_4(a_2\ell_{11}U_2 - \overline{U}_1V_1V_2)V_3V_4}{a_4\ell_{12}\ell_{71}V_2},$$

$$q_7 = -\frac{\overline{U}_4(a_2\ell_{11}U_2 - \overline{U}_1V_1V_2)V_4}{a_4\ell_{12}V_2}, \quad q_8 = \frac{-a_2\ell_{11}U_2 + \overline{U}_1V_1V_2}{\ell_{12}V_2},$$

$$q_1^* = 1, \quad q_2^* = \frac{U_2\overline{V}_1}{a_2}, \quad q_3^* = \frac{U_2U_3(-a_2\ell_{11}\overline{U}_1\overline{U}_2 + \overline{V}_1\overline{V}_2)}{a_2\ell_{31}},$$

$$q_4^* = \frac{U_2U_3U_4\overline{V}_3(-a_2\ell_{11}\overline{U}_1\overline{U}_2 + \overline{V}_1\overline{V}_2)}{a_2a_4\ell_{31}}, \quad q_5^* = \frac{U_1U_2U_3U_4\overline{V}_3\overline{V}_4(-a_2\ell_{11}\overline{U}_1\overline{U}_2 + \overline{V}_1\overline{V}_2)}{a_2a_4\ell_{31}\ell_{52}},$$

$$q_6^* = \frac{U_3U_4(a_4^2\ell_{12}\ell_{71}\overline{U}_1\overline{U}_3^2\overline{U}_4^2 + \frac{U_2\ell_{51}\overline{V}_3^2\overline{V}_4^2(-a_2\ell_{11}\overline{U}_1\overline{U}_2+\overline{V}_1\overline{V}_2)}{a_2\ell_{31}\ell_{52}})}{a_4\overline{V}_2\overline{V}_3\overline{V}_4},$$

$$q_7^* = \frac{a_4\ell_{12}\overline{U}_1\overline{U}_4}{\overline{V}_3\overline{V}_4}, \quad q_8^* = \frac{\ell_{12}\overline{U}_1}{\overline{V}_4},$$

where $U_j = \mathrm{e}^{-\mathrm{i}w_c\tau_j}$, $V_j = \mathrm{i}w_c + d_j$, for $j = 1, 2, 3, 4$. If we take $\bar{\rho}$ to be

$$(q_1\overline{q_1^*} + q_2\overline{q_2^*} + \cdots + q_8\overline{q_8^*}) + J_1\tau_1\mathrm{e}^{-\mathrm{i}w_c\tau_1} + J_2\tau_2\mathrm{e}^{-\mathrm{i}w_c\tau_2} + J_3\tau_3\mathrm{e}^{-\mathrm{i}w_c\tau_3} + J_4\tau_4\mathrm{e}^{-\mathrm{i}w_c\tau_4}, \tag{3.29}$$

where $J_1 := \ell_{11}q_2\overline{q_1^*} + \ell_{12}q_8\overline{q_1^*} + \ell_{52}q_4\overline{q_5^*} + \ell_{51}q_6\overline{q_5^*}$, $J_2 := a_2(q_1\overline{q_2^*} + q_5\overline{q_6^*})$, $J_3 := \ell_{31}q_2\overline{q_3^*}+\ell_{71}q_6\overline{q_7^*}$ and $J_4 := a_4(q_3\overline{q_4^*}+q_7\overline{q_8^*})$, then $\langle q^*, q\rangle = 1$ and $\langle q^*, \bar{q}\rangle = 0$; see appendix A.

Next, we use q and q^* to construct a coordinate for the center manifold Ω_0 at $\mu = 0$. Let $\mathbb{X}_t = \mathbb{X}_t(\theta) = (x_{1,t}(\theta), \ldots, x_{4,t}(\theta), y_{1,t}(\theta), \ldots, y_{4,t}(\theta))^{\mathrm{T}}$ be a solution of (3.26), and let

$$z(t) := \langle q^*,\ \mathbb{X}_t\rangle, \tag{3.30}$$

$$W(t,\theta) := \mathbb{X}_t(\theta) - 2\mathrm{Re}(z(t)q(\theta)). \tag{3.31}$$

On the center manifold Ω_0, $W(t,\theta) = W(z(t), \bar{z}(t), \theta)$. By the tangency to the center eigenspace at the equilibrium, we have

$$W(t,\theta) = W(z(t),\bar{z}(t),\theta) = W_{20}(\theta)\frac{z^2(t)}{2} + W_{11}(\theta)z(t)\bar{z}(t) + W_{02}(\theta)\frac{\bar{z}^2(t)}{2} + \cdots, \tag{3.32}$$

where z and $\bar{z}$ are the local coordinates of the center manifold Ω_0 in directions q^* and $\overline{q^*}$, respectively.

For the solution $\mathbb{X}_t \in \Omega_0$ of (3.26), at $\mu = 0$, we have

$$\begin{aligned}
\dot{z} =\ & \langle q^*, \dot{\mathbb{X}}_t\rangle \\
=\ & \langle q^*, A\mathbb{X}_t\rangle + \langle q^*, R_0\mathbb{X}_t\rangle \\
=\ & \langle A^*q^*, \mathbb{X}_t\rangle + \langle q^*, R_0\mathbb{X}_t\rangle \\
=\ & \langle -\mathrm{i}w_cq^*, \mathbb{X}_t\rangle + \langle q^*(0)\mathrm{e}^{\mathrm{i}w_c\theta}, R_0\mathbb{X}_t\rangle \\
=\ & \mathrm{i}w_cz + \overline{q^*}^{\mathrm{T}}(0)G_0(\mathbb{X}_t) \\
=\ & \mathrm{i}w_cz + \overline{q^*}^{\mathrm{T}}(0)G_0(W(z,\bar{z},\cdot) + 2\mathrm{Re}(zq(\cdot))) \\
=:\ & \mathrm{i}w_cz + \overline{q^*}^{\mathrm{T}}(0)\,f_0(z,\bar{z}).
\end{aligned}$$

Therefore,

$$\dot{z}(t) = \mathrm{i}w_cz(t) + g(z(t),\bar{z}(t)), \tag{3.33}$$

where $g(z(t),\bar{z}(t)) := \overline{q^*}^{\mathrm{T}}(0)\,f_0(z(t),\bar{z}(t))$. Next, we expand g in powers of z and $\bar{z}$:

$$g(z,\bar{z}) = g_{20}\frac{z^2}{2} + g_{11}z\bar{z} + g_{02}\frac{\bar{z}^2}{2} + g_{21}\frac{z^2\bar{z}}{2} + \cdots. \tag{3.34}$$

From the coefficients g_{20}, g_{11}, g_{02} and g_{21}, we shall compute the values of ν_2, ζ_2 and T_2 which are needed to determine the direction, stability and period of the periodic solution in Hopf bifurcation theorem. Note that $g(z,\bar{z}) = \overline{q^*}^{\mathrm{T}}(0)G_0(\mathbb{X}_t)$. Hence, by (3.34), we can derive

$$\begin{aligned}
g_{20} =\ & \frac{2}{\bar{\rho}}\{\mathrm{e}^{-2\mathrm{i}w_c\tau_1}[(m_{11}q_2^2 + q_8(m_{12}q_2 + m_{13}q_8))\overline{q_1^*} + (m_{53}q_4^2 + q_6(m_{52}q_4 + m_{51}q_6))\overline{q_5^*}] \\
& + \mathrm{e}^{-2\mathrm{i}w_c\tau_3}(m_{31}q_2^2\overline{q_3^*} + m_{71}q_6^2\overline{q_7^*})\}, \\
g_{11} =\ & \frac{1}{\bar{\rho}}\{(m_{12}q_2 + 2m_{13}q_8)\bar{q}_8\overline{q_1^*} + \bar{q}_2[(2m_{11}q_2 + m_{12}q_8)\overline{q_1^*} + 2m_{31}q_2\overline{q_3^*}] \\
& + (2m_{53}q_4\overline{q_4} + m_{52}q_6\bar{q}_4 + m_{52}q_4\bar{q}_6 + 2m_{51}q_6\bar{q}_6)\overline{q_5^*} + 2m_{71}q_6\bar{q}_6\overline{q_7^*}\},
\end{aligned}$$

$$
\begin{aligned}
g_{02} = {} & \frac{2}{\bar{\rho}}\{\mathrm{e}^{2\mathrm{i}w_c\tau_1}[(m_{11}\bar{q}_2^2 + m_{12}\bar{q}_2\bar{q}_8 + m_{13}\bar{q}_8^2)\overline{q_1^*} + (m_{53}\bar{q}_4^2 + m_{52}\bar{q}_4\bar{q}_6 + m_{51}\bar{q}_6^2)\overline{q_5^*}] \\
& + \mathrm{e}^{2\mathrm{i}w_c\tau_3}(m_{31}\bar{q}_2^2\overline{q_3^*} + m_{71}\bar{q}_6^2\overline{q_7^*})\}, \\
g_{21} = {} & \frac{1}{\bar{\rho}}\{\mathrm{e}^{-\mathrm{i}w_c\tau_3}[2q_2\overline{q_3^*}(3m_{32}q_2\bar{q}_2 + 2m_{31}W_{11}^{(2)}(-\tau_3)) + 2q_6\overline{q_7^*}(3m_{72}q_6\bar{q}_6 + 2m_{71}W_{11}^{(6)}(-\tau_3))] \\
& + 2\mathrm{e}^{-\mathrm{i}w_c\tau_1}[\overline{q_5^*}((3m_{57}q_4^2 + q_6(2m_{56}q_4 + m_{55}q_6))\bar{q}_4 + (m_{56}q_4^2 + 2m_{55}q_4q_6 + 3m_{54}q_6^2)\bar{q}_6 \\
& + (2m_{53}q_4 + m_{52}q_6)W_{11}^{(4)}(-\tau_1) + (m_{52}q_4 + 2m_{51}q_6)W_{11}^{(6)}(-\tau_1)) \\
& + \overline{q_1^*}((3m_{14}q_2^2 + q_8(2m_{15}q_2 + m_{16}q_8))\bar{q}_2 + (m_{15}q_2^2 + 2m_{16}q_2q_8 + 3m_{17}q_8^2)\bar{q}_8 \\
& + (2m_{11}q_2 + m_{12}q_8)W_{11}^{(2)}(-\tau_1) + (m_{12}q_2 + 2m_{13}q_8)W_{11}^{(8)}(-\tau_1))] \\
& + 2\mathrm{e}^{\mathrm{i}w_c\tau_3}(m_{31}\bar{q}_2\overline{q_3^*}W_{20}^{(2)}(-\tau_3) + m_{71}\bar{q}_6\overline{q_7^*}W_{20}^{(6)}(-\tau_3)) \\
& + \mathrm{e}^{\mathrm{i}w_c\tau_1}[\overline{q_5^*}((2m_{53}\bar{q}_4 + m_{52}\bar{q}_6)W_{20}^{(4)}(-\tau_1) + (m_{52}\bar{q}_4 + 2m_{51}\bar{q}_6)W_{20}^{(6)}(-\tau_1)) \\
& + \overline{q_1^*}((2m_{11}\bar{q}_2 + m_{12}\bar{q}_8)W_{20}^{(2)}(-\tau_1) + (m_{12}\bar{q}_2 + 2m_{13}\bar{q}_8)W_{20}^{(8)}(-\tau_1))]\}, \qquad (3.35)
\end{aligned}
$$

where $W_{20}^{(k)}(\theta)$, $W_{11}^{(k)}(\theta)$ and $W_{02}^{(k)}(\theta)$ are the kth components of $W_{20}(\theta)$, $W_{11}(\theta)$ and $W_{02}(\theta)$, respectively; see appendix B.

In the following, we shall calculate the values of $W_{20}(\theta)$ and $W_{11}(\theta)$, and substitute these values into (3.35) to calculate g_{21}; the detailed computation is arranged in appendix C. By the definition of A in (3.24), and comparing the coefficients in $\dot{W} = \dot{\mathbb{X}}_t - \dot{z}q(\theta) - \dot{\bar{z}}\bar{q}(\theta)$ with the ones of $\dot{W} = W_z\dot{z} + W_{\bar{z}}\dot{\bar{z}}$, we obtain, for $-\tau_M \leqslant \theta < 0$,

$$
\begin{aligned}
AW_{20}(\theta) &= \dot{W}_{20}(\theta) = 2\mathrm{i}w_cW_{20}(\theta) + g_{20}q(\theta) + \bar{g}_{02}\bar{q}(\theta), \\
AW_{11}(\theta) &= \dot{W}_{11}(\theta) = g_{11}q(\theta) + \bar{g}_{11}\bar{q}(\theta).
\end{aligned} \qquad (3.36)
$$

For $-\tau_M \leqslant \theta < 0$, the solution of (3.36) is

$$
\begin{aligned}
W_{20}(\theta) &= \frac{\mathrm{i}g_{20}}{w_c}q(0)\mathrm{e}^{\mathrm{i}w_c\theta} - \frac{\bar{g}_{02}}{3\mathrm{i}w_c}\bar{q}(0)\mathrm{e}^{-\mathrm{i}w_c\theta} + E_1\mathrm{e}^{2\mathrm{i}w_c\theta}, \\
W_{11}(\theta) &= \frac{g_{11}}{\mathrm{i}w_c}q(0)\mathrm{e}^{\mathrm{i}w_c\theta} - \frac{\bar{g}_{11}}{\mathrm{i}w_c}\bar{q}(0)\mathrm{e}^{-\mathrm{i}w_c\theta} + E_2,
\end{aligned} \qquad (3.37)
$$

where

$$
E_1 = (2\mathrm{i}w_cI - \int_{-\tau_M}^{0}\mathrm{e}^{2\mathrm{i}w_c\theta}\,\mathrm{d}\eta(\theta,0))^{-1}\begin{pmatrix} 2\mathrm{e}^{-2\mathrm{i}w_c\tau_1}(m_{11}q_2^2 + q_8(m_{12}q_2 + m_{13}q_8)) \\ 0 \\ 2\mathrm{e}^{-2\mathrm{i}w_c\tau_3}m_{31}q_2^2 \\ 0 \\ 2\mathrm{e}^{-2\mathrm{i}w_c\tau_1}(m_{53}q_4^2 + q_6(m_{52}q_4 + m_{51}q_6)) \\ 0 \\ 2\mathrm{e}^{-2\mathrm{i}w_c\tau_3}m_{71}q_6^2 \\ 0 \end{pmatrix}, \qquad (3.38)
$$

$$
E_2 = \left(-\int_{-\tau_M}^{0}\mathrm{d}\eta(\theta,0)\right)^{-1}\begin{pmatrix} 2m_{11}|q_2|^2 + 2m_{12}\mathrm{Re}(q_8\bar{q}_2) + 2m_{13}|q_8|^2 \\ 0 \\ 2m_{31}|q_2|^2 \\ 0 \\ 2m_{53}|q_4|^2 + 2m_{52}\mathrm{Re}(q_6\bar{q}_4) + 2m_{51}|q_6|^2 \\ 0 \\ 2m_{71}|q_6|^2 \\ 0 \end{pmatrix}. \qquad (3.39)
$$

Next we substitute $W_{20}(\theta)$ and $W_{11}(\theta)$ into (3.35) to obtain g_{21}. Finally, we can use these computations of g_{20}, g_{11}, g_{02} and g_{21} to obtain the following quantities

$$\begin{aligned}
C_1(0) &= \frac{\mathrm{i}}{2w_c}(g_{20}g_{11} - 2|g_{11}|^2 - \frac{1}{3}|g_{02}|^2) + \frac{g_{21}}{2},\\
\nu_2 &= -\frac{\mathrm{Re}(C_1(0))}{\mathrm{Re}(\lambda'(r_c))},\\
\zeta_2 &= 2\mathrm{Re}(C_1(0)),\\
T_2 &= \frac{-1}{w_c}[\mathrm{Im}(C_1(0)) + \nu_2\mathrm{Im}(\lambda'(r_c))];
\end{aligned}$$

cf [15]. By theorem 3.2 and proposition 3.5, we draw the following conclusions.

Theorem 3.6. *For a fixed $s \geqslant 0$, assume that (3.9) or (3.10) and (3.17), (3.20), and conditions (B1), (B2) hold. Then system (2.5) undergoes a Hopf bifurcation at $r = r_c$ ($\mu = 0$) and $\overline{\mathbb{X}} = 0$. More precisely,*

(i) The direction of the Hopf bifurcation is determined by the sign of ν_2. If $\nu_2 > 0$ (respectively, < 0), it is supercritical (respectively, subcritical) and a bifurcated periodic solution exists for $r > r_c$ (respectively, $r < r_c$) with r near r_c.

(ii) The stability of the bifurcated periodic solution is determined by the sign of ζ_2. If $\zeta_2 < 0$ (respectively, > 0), then the periodic solution is stable (respectively, unstable).

(iii) The period of the bifurcated periodic solution is determined by the sign of T_2. If $T_2 > 0$ (respectively, < 0) and $\nu_2 > 0$, then the period increases (respectively, decreases) as μ increases. If $T_2 < 0$ (respectively, > 0) and $\nu_2 < 0$, then the period increases (respectively, decreases) as μ decreases.

According to theorems 3.2 and 3.6, we summarize the respective criteria for the stable synchronous and asynchronous oscillations.

Condition (S): (3.9) or (3.10) holds, $Q_+(w_c) = \Gamma$, (3.17), (3.20), and conditions (B1), (B2) hold, and $\zeta_2 < 0$.
Condition (AS): (3.9) or (3.10) holds, $Q_-(w_c) = \Gamma$, (3.17), (3.20), and conditions (B1), (B2) hold, and $\zeta_2 < 0$.

Corollary 3.7. *If condition (S) (respectively, (AS)) holds for parameters (a_2, d_1, d_2, k_H, P_0, a_4, d_3, d_4, k_D, P_{D_0}) and a fixed $s \geqslant 0$, then there exists a stable synchronous (respectively, asynchronous) periodic solution of system (2.5), for $|r - r_c|$ small and $r > r_c$, if $\nu_2 > 0$, and $r < r_c$, if $\nu_2 < 0$.*

4. Collective behaviour and numerical illustrations

We summarize the theories established in previous sections and delineate the chief dynamics regimes of system (1.1) in section 4.1. In section 4.2, we provide three numerical examples to demonstrate our theories and illustrate the dynamical scenario exhibited by the considered model.

4.1. Collective behaviour

According to the analysis in previous sections, β_4, the product of all degradation rates d_i, $i = 1, 2, 3, 4$, organizes the dynamics of system (1.1). Recall remark 3.1(iii), (2.10) and (3.9) and note that $\rho_1 \geqslant \gamma_1$, $\rho_2 \geqslant \gamma_2$, and $\rho_3 \geqslant \gamma_3$ yield $a_2d_3d_4\gamma_1 + a_2a_4\gamma_2\gamma_3 \leqslant a_2d_3d_4\rho_1 + a_2a_4\rho_2\rho_3$.

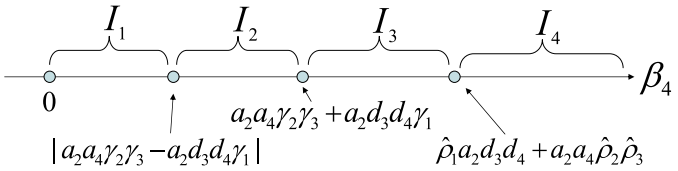

Figure 2. Partition for the range of β_4: $I_1 = (0, |a_2a_4\gamma_2\gamma_3 - a_2d_3d_4\gamma_1|)$, $I_2 = (|a_2a_4\gamma_2\gamma_3 - a_2d_3d_4\gamma_1|, a_2a_4\gamma_2\gamma_3 + a_2d_3d_4\gamma_1)$, $I_3 = (a_2a_4\gamma_2\gamma_3 + a_2d_3d_4\gamma_1, \hat{\rho}_1a_2d_3d_4 + a_2a_4\hat{\rho}_2\hat{\rho}_3)$, $I_4 = (\hat{\rho}_1a_2d_3d_4 + a_2a_4\hat{\rho}_2\hat{\rho}_3, \infty)$; $\hat{\rho}_i$ is defined in (2.11), $i = 1, 2, 3$.

We depict in figure 2 a typical dynamical scenario for (1.1) as β_4 increases from zero to ∞, based on both theoretical and numerical supports.

(D1) If $\beta_4 \in I_1$, then (3.10) holds and both $Q_+(w) = \Gamma$ and $Q_-(w) = \Gamma$ have solutions, by lemma 3.1. Therefore, if conditions $(C1)_\sigma$ and $(C2)_\sigma$ hold at some w_σ and $r_\sigma^{(k)}$ for some $k \in \mathbb{Z}$, $\sigma = +$ or $-$, then r-induced synchronous (respectively, asynchronous) oscillation is generated, for r near $r_+^{(k)}$ (respectively, $r_-^{(k)}$).

(D2) If $\beta_4 \in I_1 \cup I_2$, then (3.9) holds and $Q_+(w) = \Gamma$ has a solution. Hence, if conditions $(C1)_+$ and $(C2)_+$ hold at some w_+ and $r_+^{(k)}$ for some $k \in \mathbb{Z}$, then the r-induced synchronous oscillation is generated, for r near $r_+^{(k)}$. In addition, if $\beta_4 \in I_2$, then $Q_-(w) = \Gamma$ may or may not have a solution. We do find numerical examples with $\beta_4 \in I_2$ (purple region in example 4.1) so that $Q_+(w) = \Gamma$ has a solution, but $Q_-(w) = \Gamma$ does not.

(D3) If $\beta_4 \in I_3$, then both $Q_+(w) = \Gamma$ and $Q_-(w) = \Gamma$ do not have any solution and the system is non-oscillatory, according to our numerical computations.

(D4) If $\beta_4 \in I_4$, then according to remark 2.2(i), the system achieves global convergence to the unique synchronous equilibrium $\bar{\mathbb{X}}$. Therefore, there does not exist any oscillation.

From figure 2, we observe that large degradation rates lead to oscillation-arrested.

4.2. Numerical illustrations

The analytic theories presented in theorem 2.6 and corollary 3.7 have provided the criteria for oscillation-arrested, synchronous and asynchronous oscillations of system (1.1). Those criteria consist of inequalities involving the parameters and delays and can be examined numerically. As indicated in corollary 3.7, the synchronization depends on several factors including the magnitudes of degradation rates and delays. To elucidate more concretely the dynamics regimes asserted in these theories, we present example 4.1 which provides a graphic illustration through examining these criteria and demonstrate the dynamics through solving the delay differential equations (1.1) numerically. In example 4.2, we illustrate the dynamics with parameters and delays adopted in [25]. The dynamics of system (1.1) describes the collective behaviour for two cells in contact in the PSM and actually does not incorporate the spatial structure. That is, the positions for the cells are regarded fixed. However, as the embryo grows, the PSM boundary shifts posteriorly, and the position of the considered cells moves from the posterior PSM to the anterior PSM. The cells experience different stages during the process. We thereby compose a system, arranged in example 4.3, with multiple phases, namely, synchronous oscillation, oscillation slowing down and oscillation-arrested, to delineate the phase transition of two adjacent cells in the PSM.

The following parameters are adopted in [25]:

$$a_2 = 4.5, \quad a_4 = 4.5, \quad k_D = 33, \quad k_H = 33, \quad P_0 = 40, \quad P_{D_0} = 400, \tag{4.1}$$
$$d_1 = 0.252525, \quad d_2 = 0.23, \quad d_3 = 0.273224, \quad d_4 = 0.23.$$

From the experiment in [12], the delay magnitudes considered in [25] are

$$\begin{aligned} &\tau_1 = 3.8 \pm 1.0 + T_{\text{init-her}}, && \tau_3 = 8.4 \pm 1.2 + T_{\text{init-delta}}, \\ &\tau_2 \approx 2.8, && \tau_4 \approx 20, \end{aligned} \tag{4.2}$$

where the unit of time delay is minute. The symbol '$\pm$' in (4.2) means the error of the mean, and $T_{\text{init-her}}$ (respectively, $T_{\text{init-delta}}$) is the time for bound inhibitory protein and for the mRNA polymerase to produce sufficient transcription for *her1* (respectively, *delta*) gene. The values $T_{\text{init-her}} = T_{\text{init-delta}} = 4$ were adopted in [25].

On the other hand, Lewis [21] denoted by T_N the total time delay during the Notch signalling pathway, which is separated into four parts:

$$T_N = T_{\text{mdeltaC}} + T_{\text{pdeltaC}} + T_{\text{pexport}} + T_{\text{NotchActivation}},$$

where T_{mdeltaC} is the delay for *delta* gene transcription (between 16 and 68 min), T_{pdeltaC} is the delay for *delta* gene translation (about 5.5 min), T_{pexport} is the delay for delivery of the protein via the secretory pathway to the cell membrane (about 15 min), and $T_{\text{NotchActivation}}$ is the delay for the resultant activated Notch arriving in the nucleus of the neighbouring cell, which is short compared to T_{pexport}. In our notation, τ_3 and τ_4 correspond to T_{mdeltaC} and $T_{\text{pdeltaC}} + T_{\text{pexport}}$, respectively. In particular, τ_4 represents the total delay for making a mature molecule of Delta protein via translation and delivery to the cell membrane. Therefore, if $T_{\text{NotchActivation}}$ is very small or is included in τ_1, then T_N can be regraded as our $s = \tau_3 + \tau_4$. Hence, we regard s as the role of T_N in the following examples. We use Mathematica and Matlab software in the following computations.

Example 4.1. In this example, we illustrate the dynamics regimes through examining the criteria established in theorem 2.6 and corollary 3.7, then we justify these dynamics through solving delay differential equations (1.1) numerically. For system (1.1) with the parameters in (4.1), we further set $\tau_2 = 2.8$, $\tau_4 = 20$, and $d_1 = d_2 = d_3 = d_4 = d_*$ for $d_* \geqslant 0.01$. The degradation rates are set equal for demonstration purpose. We vary the values of d_* and $s = \tau_3 + \tau_4$ to examine whether the parameters and delays satisfy the criteria for the chief dynamics of (1.1). In doing so, we shall provide a visual illustration to see how dynamics regimes vary with respect to d_* and s. More precisely, we consider (1.1) with the value of d_* increasing from 0.01 to 2.4 with increment 0.01 and the value of s from 21 to 105 (i.e. τ_3 from 1 to 85) with increment 1 successively. In figure 3, the colours mark the values of (d_*, s), and system (1.1) admits identical properties under values (d_*, s) at the locations of the same colour. The green dot means the parameters satisfy $\beta_4 \geqslant a_2a_4\gamma_2\gamma_3 + a_2d_3d_4\gamma_1$, i.e. they do not satisfy (3.9), which is a sufficient condition for the existence of purely imaginary root of $\Delta_+(\cdot, r, s) = 0$. In fact, according to our numerical computation, there is no solution to $Q_+(w) = \Gamma$ and $Q_-(w) = \Gamma$. The dark green dot means that the parameters satisfy (2.12), i.e. the corresponding system admits global convergence to the unique equilibrium $\bar{\mathbb{X}}$. The light blue dot means there exists a root $\mathrm{i}w_c$ of $\Delta_+(\cdot, r_c, s) = 0$ and the values of the terms in the transversality condition $(\text{C2})_+$ are small at w_c and r_c. The orange dot means that there is a root $\mathrm{i}w_c$ of $\Delta_-(\cdot, r_c, s) = 0$ and the values of the terms in the transversality condition $(\text{C2})_-$ are low at w_c and r_c. The blue dot means both $Q_+(w) = \Gamma$ and $Q_-(w) = \Gamma$ have solutions, and condition (S) holds, i.e. there exists a stable synchronous periodic solution for r near r_c. The pink dot means condition (AS) holds, i.e. there exists a stable asynchronous periodic solution for r near r_c. The purple dot means only $Q_+(w) = \Gamma$ has a solution, but $Q_-(w) = \Gamma$ does not have any solution, and condition (S) holds, i.e. there exists only synchronous periodic solution and does not exist any bifurcated asynchronous periodic solution. The grey dot indicates that the magnitudes of $D_3^{\pm}$ and $D_4^{\pm}$ in (3.16) are smaller than our working precision. The black dot means the parameters satisfy (3.9) and there exist purely imaginary characteristic values w_+

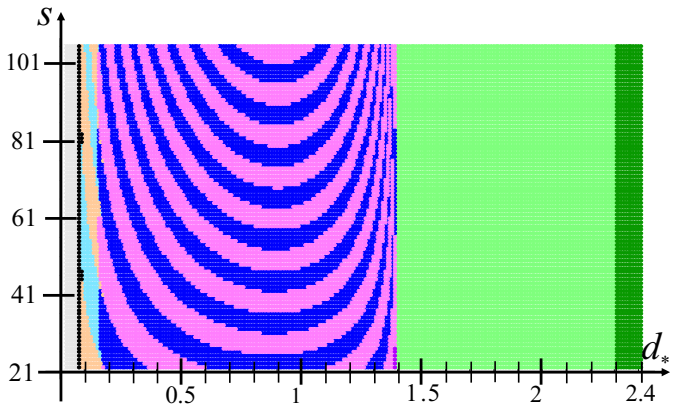

Figure 3. The colours mark the values of (d_*, s). System (1.1) admits identical properties under values (d_*, s) of the same colour.

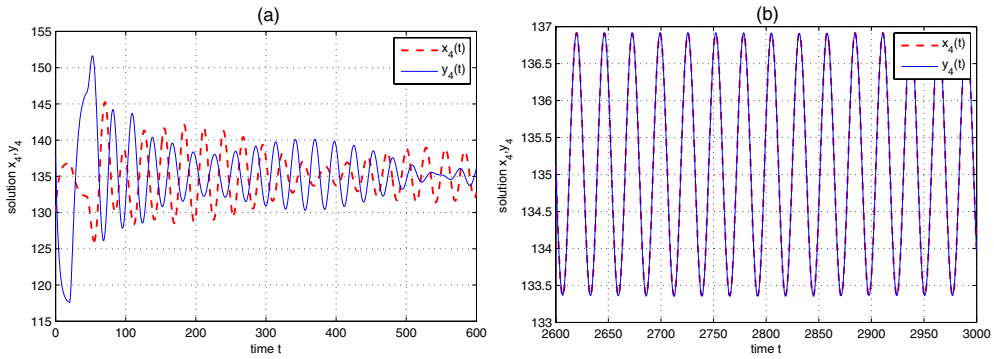

Figure 4. Evolution of $x_4(t)$, $y_4(t)$, for (a) $t \in [0, 600]$, (b) $t \in [2600, 3000]$, with $(d_*, s) = (0.23, 44)$, $\tau_1 = 3.90264$, $\tau_3 = 24$ and $r = 6.70264$ near r_c, which satisfy condition (S). The solution tends to a stable synchronous periodic solution with period 27.

which are smaller than our working precision. We do not consider these parameters represented by black and grey dots in the following discussions. According to corollary 3.7, if condition (S) or (AS) holds, then we compute w_c and r_c which are dependent on s. In the numerical computation, τ_1 is then chosen to be near $(r_c - 2.8)$.

Next, we elucidate the dynamics in detail for the parameters located at various colours in figure 3. In figures 4–7, we only demonstrate the solution evolved from the constant initial value $\phi = (10, 180, 7, 130, 8, 170, 6, 138)$ and its $x_4(t)$ and $y_4(t)$ components.

(I) For (d_*, s) lying in the blue (respectively, pink) region of figure 3, the system satisfies condition (S) (respectively, (AS)), and there exists a stable synchronous (respectively, asynchronous) periodic solution bifurcated from equilibrium $\bar{\mathbb{X}}$, for r near r_c, by corollary 3.7. The dynamics for (1.1) with these parameters are computed numerically in figure 4 (respectively, figure 6).

(II) Consider again (d_*, s) lying in the blue region and the pink region of figure 3, respectively. We demonstrate theorem 3.2 numerically. For any given $s \geqslant 0$, all purely imaginary roots $\mathrm{i}w_\pm$ of $\Delta(\cdot, r, s) = 0$ can be computed numerically. For each $w_\pm$, there exists a sequence

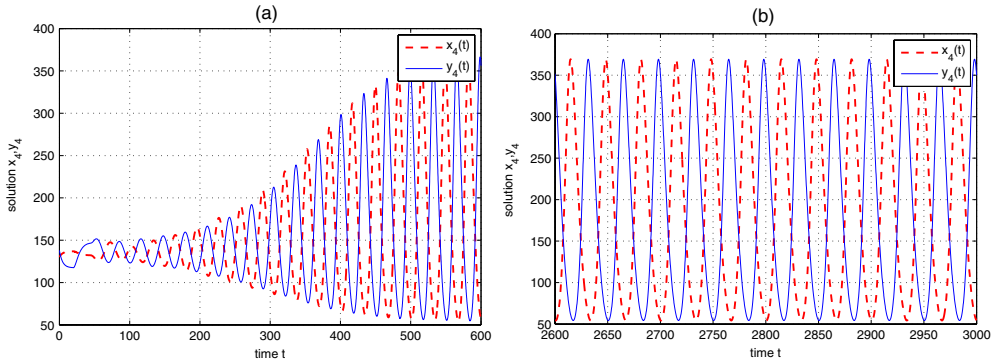

Figure 5. Dynamics of $x_4(t)$, $y_4(t)$, for (a) $t \in [0, 600]$, (b) $t \in [2600, 3000]$, with $(d_*, s) = (0.23, 44)$, $\tau_1 = 5.543\,09$, $\tau_3 = 24$, and $r = 8.343\,09$ near certain bifurcation value larger than r_c. The solution tends to an asynchronous periodic solution with period 33.

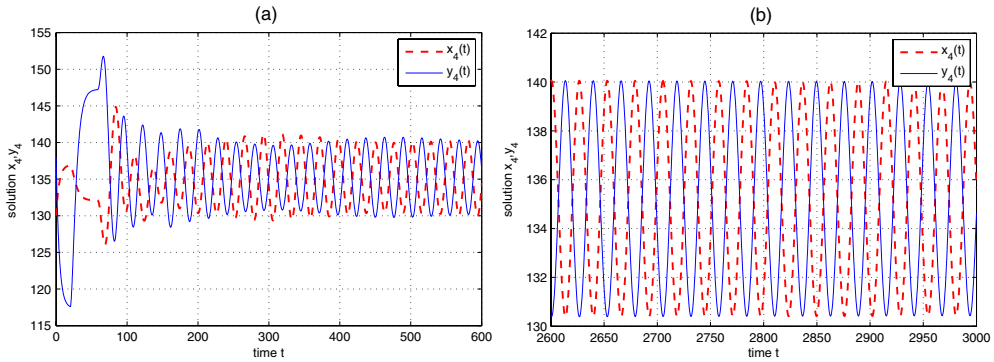

Figure 6. Evolution of $x_4(t)$, $y_4(t)$, for (a) $t \in [0, 600]$, (b) $t \in [2600, 3000]$, with $(d_*, s) = (0.23, 58)$, $\tau_1 = 3.669\,71$, $\tau_3 = 38$, and $r = 6.469\,71$ near r_c, which satisfy condition (AS). The solution tends to a stable asynchronous periodic solution with period 26.

$\{r_\pm^{(k)}(w_\pm)\}$ such that the system has a periodic solution, at r near the bifurcation value $r_\pm^{(k)}(w_\pm)$, if conditions $(C1)_\pm$ and $(C2)_\pm$ hold at $w_\pm$ and $r_\pm^{(k)}(w_\pm)$, for some $k \in \mathbb{Z}$. In figure 5, we take $r = 8.343\,09$, which is near certain bifurcation value larger than the smallest bifurcation value r_c chosen in figure 4; an asynchronous periodic orbit emerges, in contrast to the synchronous one in figure 4.

(III) Figures 4, 5, 6 and 7 demonstrate that, as the bifurcation value r increases, the system undergoes a sequence of phase exchanges between synchronous oscillation and asynchronous oscillation. This illustrates a scenario on how $r = \tau_1 + \tau_2$, the delay for *her* gene, affects the synchronization. In addition, observe figures 4 and 6, which have the same d_* but different s. It also undergoes a sequence of phase exchanges between synchronous and asynchronous oscillations as s varies. This scenario shows how $s = \tau_3 + \tau_4$, the delay for *delta* gene, affects the synchronization. Indeed, synchrony of periodic orbit can be broken by choosing inappropriate values of r or s.

(IV) We connect the dynamics regimes depicted in figure 2 with the numerics in this example. Recall the intervals I_1, I_2, I_3, I_4 in figure 2. First, for any $s \geqslant 0$, if $d_* \geqslant 0.07$, then the parameters satisfy (3.17) and (3.20). So we only consider $d_* \geqslant 0.07$. In this range, there is a correspondence between the values of β_4 and d_*; namely, for any fixed $s \geqslant 0$, if $d_* \in \{0.07, 0.08, \ldots, 1.24, 1.25\}$ and $d_* \in \{1.26, 1.27, \ldots, 1.37, 1.38\}$, then $\beta_4 \in I_1$ and

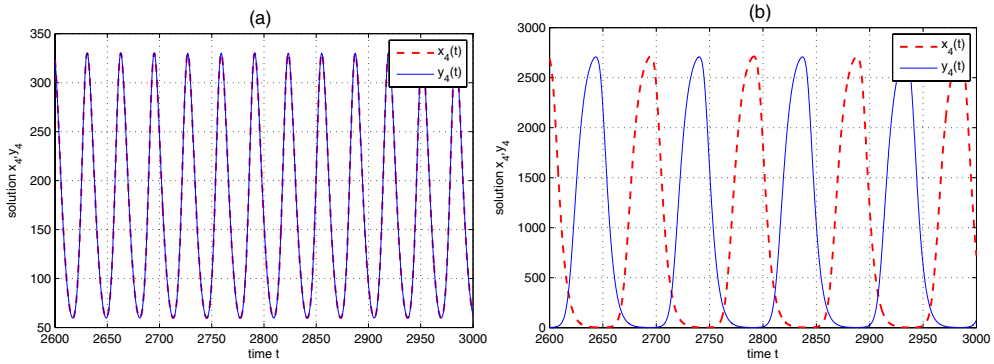

Figure 7. Evolutions of $x_4(t)$, $y_4(t)$ for $t \in [2600, 3000]$, with (d_*, s), τ_3 as in figure 6, and (*a*) $\tau_1 = 5.17878$, $r = 7.97878$, (*b*) $\tau_1 = 33.0221$, $r = 35.8221$. The oscillation switches from asynchrony in figure 6 to synchrony in (*a*), then to asynchrony in (*b*).

$\beta_4 \in I_2$, respectively. The dynamics of these two regions correspond to (D1) and (D2). The equilibrium $\bar{\mathbb{X}}$ of system (1.1) is asymptotically stable, for any $s \geqslant 0$ and $r < r_c$, by proposition 3.5. If $d_* \in \{2.3, 2.31, \ldots, 2.39, 2.4\}$, then $\beta_4 \in I_4$, and system (1.1) admits the global convergence to equilibrium $\bar{\mathbb{X}}$, which is associated with the dynamics depicted in (D4), by remark 2.2 (i). Finally, if $d_* \in \{1.39, 1.4, \ldots, 2.28, 2.29\}$, then $\beta_4 \in I_3$ and both $Q_+(w) = \Gamma$ and $Q_-(w) = \Gamma$ do not have any solution, according to the numerical computation. Hence, Hopf bifurcation theory is not applicable for the parameters in this range. In fact, these parameters belong to the green region in figure 3, and the equilibrium $\bar{\mathbb{X}}$ is asymptotically stable, for any $s \geqslant 0$ and $r \geqslant 0$, by remark 3.3(ii).

(V) In the regime of synchronous oscillation, we can also examine the periods of oscillations corresponding to various parameters and delays, through further numerical computation. To this end, we focus on those parameters and delays which satisfy condition (S), i.e. the blue and purple regions in figure 3. If we fix $d_* \in \{0.15, 0.16, \ldots, 1.29, 1.3\}$ and vary $s \in \{21, 22, \ldots, 104, 105\}$, then the periods of the corresponding periodic solutions are almost the same. This indicates that s, the delay for Notch signalling pathway, has a mild effect on the period in this regime. On the other hand, if $d_* \in \{1.31, 1.32, \ldots, 1.37, 1.38\}$ is fixed, then the period of oscillation increases as s increases. One can also fix s, and compute how period changes with respect to d_*. Our numerical simulation shows that the period of oscillation increases as the degradation rates approach the values corresponding to the oscillation-arrest. For example, as $s = 38$, $(d_*, p) = (1.29, 19), (1.35, 35), (1.37, 38)$; as $s = 46$, $(d_*, p) = (1.24, 16), (1.32, 22), (1.37, 45)$, where p denotes the period.

Example 4.2. The parameters in (4.1) and delays in (4.2) with $T_{\text{init-her}} = T_{\text{init-delta}} = 4$, are considered in the heterodimer model in [25]. In this example, we take $\tau_2 = 2.8$, $\tau_3 = 12.4$, $\tau_4 = 20$ so that $s = \tau_3 + \tau_4 = 32.4$, and choose r or τ_1 ($r = \tau_1 + 2.8$) from our bifurcation theory. Then according to corollary 3.7, system (1.1) with these parameters and delays satisfies condition (AS) and admits a stable asynchronous oscillation for $r = 6.08948$ near r_c, i.e. $\tau_1 = 3.28948 \approx r_c - 2.8$, shown in figure 8(*a*), where the initial value is $\phi = (14, 46, 13.5, 45, 13.5, 47, 13, 42)$.

Moreover, if r is changed to $r = 66.5759$, near another bifurcation value larger than r_c, the evolution from the same initial value tends to a synchronous periodic solution shown in figure 8(*b*). Therefore, the system with the same parameters can generate both stable asynchronous and synchronous oscillations at different delays $r = \tau_1 + \tau_2$.

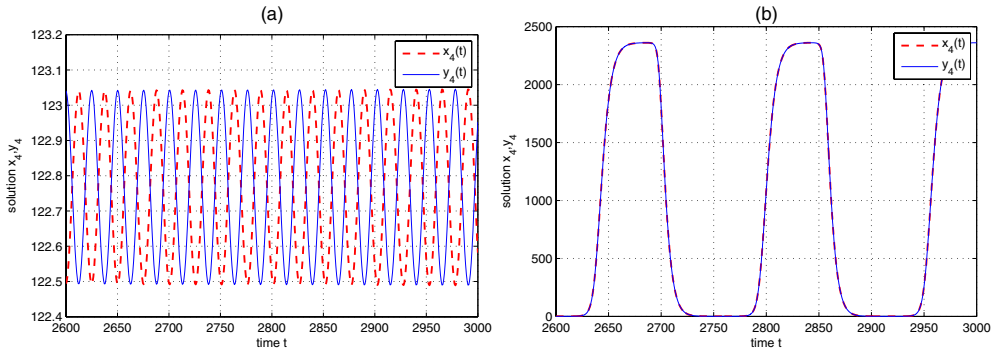

Figure 8. Evolutions of $x_4(t)$, $y_4(t)$ for $t \in [2600, 3000]$, in example 4.2; (a) asynchronous oscillation with period 25, for $r = 6.089\,48$ near r_c, which satisfies condition (AS); (b) synchronous oscillation with period 156, for $r = 66.5759$ near larger bifurcation value greater than r_c

Example 4.3. From system (1.1), we compose a non-autonomous system by choosing three parameter sets, with fixed $s = 60$ ($\tau_3 = 40$, $\tau_4 = 20$), to generate three different phases: synchronous oscillation, oscillation slowing down, and oscillation-arrested. For the first phase of synchronous oscillation, we choose

$$\begin{aligned} &a_2 = 4.5, \quad d_1 = 1.35, \quad d_2 = 1.35, \quad k_{\mathrm{H}} = 33, \quad P_0 = 40, \\ &a_4 = 4.5, \quad d_3 = 1.35, \quad d_4 = 1.35, \quad k_{\mathrm{D}} = 33, \quad P_{D_0} = 400, \end{aligned} \tag{4.3}$$

and $\tau_2 = 2.8$, which is the value adopted in [21, 25]; then by (3.13), we choose $\tau_1 = 10.4041$ so that $r = \tau_1 + \tau_2 = 13.2041$ is near r_c, i.e.

$$[\tau_1, \tau_2, \tau_3, \tau_4] = [10.4041,\ 2.8,\ 40,\ 20]. \tag{4.4}$$

For the second phase, the parameters are set as

$$\begin{aligned} &a_2 = 4.5, \quad d_1 = 1.38, \quad d_2 = 1.38, \quad k_{\mathrm{H}} = 33, \quad P_0 = 40, \\ &a_4 = 4.5, \quad d_3 = 1.38, \quad d_4 = 1.38, \quad k_{\mathrm{D}} = 33, \quad P_{D_0} = 400, \end{aligned} \tag{4.5}$$

and the delays are chosen according to (3.13),

$$[\tau_1, \tau_2, \tau_3, \tau_4] = [25.5646,\ 2.8,\ 40,\ 20]. \tag{4.6}$$

These two sets of parameters satisfy condition (S) and the period of the oscillation for the second is larger than the one for the first. Next, we choose the third set of parameters as

$$\begin{aligned} &a_2 = 4.5, \quad d_1 = 1.5, \quad d_2 = 1.5, \quad k_{\mathrm{H}} = 33, \quad P_0 = 40, \\ &a_4 = 4.5, \quad d_3 = 1.5, \quad d_4 = 1.5, \quad k_{\mathrm{D}} = 33, \quad P_{D_0} = 400, \end{aligned} \tag{4.7}$$

where the degradation rates $d_* = d_i, i = 1, 2, 3, 4$ have been increased; we retain the magnitudes of delays as (4.6). The synchronous equilibrium of system (1.1) with parameters (4.7) is

$$\bar{\mathbb{X}} = (\bar{\boldsymbol{x}}, \bar{\boldsymbol{x}}), \qquad \text{with} \quad \bar{\boldsymbol{x}} \approx (12.3262, 36.9786, 11.8622, 35.5865).$$

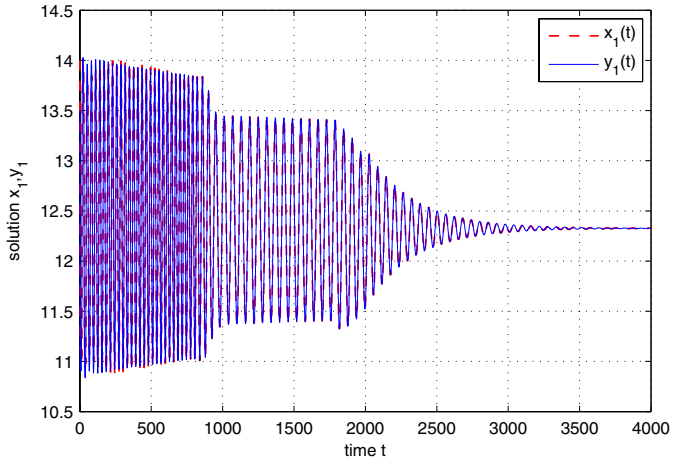

Figure 9. The x_1-, y_1-components for a non-autonomous system composed from (1.1), starting from synchronous oscillation, then slower oscillation and finally tending to the synchronous equilibrium.

In fact, the parameters in (4.7) do not satisfy condition (2.12), but satisfy the conditions in remark 3.3(ii); the system still converges to equilibrium $\bar{\mathbb{X}}$. We certainly can increase degradation rates d_* further to meet condition (2.12) and obtain a similar scenario.

The whole evolution system is then composed as follows. The parameters are set as (4.3), during $t \in [0, 800]$, and as (4.5), during $t \in [1000, 1800]$, and finally as (4.7), during $t \in [2000, 4000]$; in addition, the degradation rates increase linearly during the transition when $t \in [800, 1000] \cup [1800, 2000]$. Moreover, we set the delays equal to (4.4), when $t \in [0, 800]$, and equal to (4.6), when $t \in [1000, 4000]$; and increases linearly, when $t \in [800, 1000]$. The transitions among the settings are all continuous.

This non-autonomous system then has stable synchronous oscillation during $t \in [0, 1800]$. The period of oscillation during $t \in [0, 800]$ is about 30 min which matches the experimentally observed period for the oscillatory clock gene at the tail bud. The oscillation then slows down with the period increased and the amplitude decreased when $t \in [1000, 1800]$. Possibly due to the effect of FGF8, the cell degradation rates increase during the process. Finally, the solution tends to equilibrium $\bar{\mathbb{X}}$, when $t \in [2000, 4000]$. This phase corresponds to oscillation-arrested and the cells are formed into somites. We illustrate only the dynamics for the x_1- and y_1-components of the solution evolved from the constant initial value $\phi = (14, 46, 13.5, 45, 13.5, 47, 13, 42)$ in figure 9.

5. Discussions and conclusions

We have developed analytical theories for the kinetics of *her* gene expressions of two neighbouring cells interacted through the Delta–Notch signalling. In particular, the basic regimes of synchronous oscillation and oscillation-arrested have been identified. Our theoretical results show consistency with the numerical findings incorporated with proper biological data in [21, 25].

We found that the value of β_4, the product of all degradation rates, organizes the dynamics of system (1.1). As β_4 increases from zero, the dynamics vary from oscillatory phase to steady phase. We have proved that large degradation rates and small synthesis rates are favorable for

conditions (2.10) and (2.12) which yield global convergence to the synchronous equilibrium. This steady phase corresponds to the oscillation-arrested state for the cells in the formed somites.

This study has elucidated how synchronization and oscillation depend on the parameter values and delay magnitudes, and clarified certain assertions in the literature. For example, it was mentioned in [21] that the delay of the Notch signalling, i.e. T_N or $s = \tau_3 + \tau_4$, can synchronize *her* gene oscillations over adjacent cells. From the bifurcation analysis, we have shown that the synchrony depends on both s and r, where r is the combined delay in *her* gene regulation. In fact, holding a suitable s and varying r can lead to a sequence of phase exchanges between synchronous oscillation and asynchronous oscillation, and vice versa. It was mentioned in [28] that large coupling strength promotes the synchronization between cells. Our investigation indicated that inappropriate choice or combination of the degradation rates and the delays can destroy the synchrony even though the coupling strength, reflected in the magnitude of k_{H}, is large. Indeed, synchronous oscillation is a collective behaviour for coupled-cell system (1.1) under suitable combination of parameters and delays. Based on the present theory, we extended the investigation further through numerical simulations to depict more complete dynamical scenarios of the system. Our numerical computation indicates that under condition (S), the period of the oscillation is large, if the degradation rates are close to the values where the oscillations arrest. In addition, the period of the bifurcated periodic solution appears to be larger at larger bifurcation value.

The analytic results for the considered cell–cell system also provided a basis to compose a system with multiple phases to describe the whole evolution of two adjacent cells in the PSM during the somitogenesis. This system, presented in example 4.3, exhibits stable synchronous oscillation, oscillation with slower rate and oscillation-arrested, in succession. The formulation in turn leads to the construction of a non-autonomous lattice system of N coupled cells, which generates the travelling wave of oscillatory gene expression [23].

The established framework is rather general and can accommodate other models; for example, the heterodimer model containing *her1*, *her7* and *delta* genes, and models with Michaelis–Menten type reactions for the degradation and general transcription function with Hill coefficients. In fact, what are essentially required in our approach are the following:

(i) $\frac{\partial g_{\mathrm{H}}(u,v)}{\partial u} < 0$, $\frac{\partial g_{\mathrm{H}}(u,v)}{\partial v} > 0$ and $\frac{\mathrm{d}g_{\mathrm{D}}(u)}{\mathrm{d}u} < 0$, for all $u, v \geqslant 0$, i.e. Her protein suppresses the transcription of *her* gene, Delta protein from neighbouring cells activates the transcription of *her* gene, and Her protein suppresses the transcription of *delta* gene,

(ii) there exist constants B_1 and B_2 such that $0 < g_{\mathrm{H}}(u, v) < B_1$ and $0 < g_{\mathrm{D}}(u) < B_2$, for all $u, v \geqslant 0$, i.e. g_{H} and g_{D} are bounded,

(iii) there exists a positive synchronous equilibrium for the system.

Such g_{H} includes the one adopted in [21]:

$$g_{\mathrm{H}}(u, v) = \frac{k_{\mathrm{H}}}{1 + \frac{u^2}{P_0^2}} \times \frac{v}{P_{D_0} + v}, \qquad g_{\mathrm{D}}(u) = \frac{k_{\mathrm{D}}}{1 + \frac{u^2}{P_0^2}}.$$

Moreover, the treatment can also be applied to the system modified by adding delays in the model in [34]. Such extension responds to a research task posed in the discussion section of [34].

Furthermore, our analytic approach in concluding global convergence to the synchronous equilibrium and global synchronization can be extended to the N-cell system [23]. The basic assumption is large degradation rates. The existence of synchronous oscillation for the N-cell system is similar to the cell–cell system in section 3, as the assertion can be obtained from restricting the dynamics to the synchronous manifold, due to the symmetric coupling among

cells in the considered system. The computation for the stability of bifurcated periodic orbit is, however, more complicated, as one needs to analyze the characteristic equation obtained from the determinant of a $4N \times 4N$ matrix.

While system (1.1) models the kinetics of the gene expression in zebrafish somitogenesis, the equations actually represent typical gene regulatory networks with autorepression and time delays in transcription and translation taken into account. Mathematical analysis prevails in understanding the dynamics of the model system, and elucidates the interplay between the parameter values and delay magnitudes for the collective behaviour. However, if more genes are involved and considered in the modelling, then the size of the model system increases, so does the challenge of analysis. The mathematical analysis and technique in this study are expected to contribute toward advancing the theoretical investigation on gene regulation models including systems similar to (1.1).

Acknowledgments

The authors are grateful to Professor Yun-Jin Jiang at NHRI of Taiwan for helpful discussions on somitogenesis experiments. The authors are supported, in part, by the National Center of Theoretical Sciences and National Science Council of Taiwan.

Appendix A.

From $\langle q^*, q\rangle = 1$, we can obtain ρ as follows:

$$\begin{aligned}
\langle q^*, q\rangle &= \overline{q^*}^{\mathrm{T}}(0)q(0) - \int_{\theta=-\tau_M}^{0}\int_{\xi=0}^{\theta} \overline{q^*}^{\mathrm{T}}(\xi-\theta)\mathrm{d}\eta(\theta)q(\xi)\,\mathrm{d}\xi \\
&= \frac{1}{\bar\rho}(q_1\overline{q_1^*} + q_2\overline{q_2^*} + q_3\overline{q_3^*} + q_4\overline{q_4^*} + q_5\overline{q_5^*} + q_6\overline{q_6^*} + q_7\overline{q_7^*} + q_8\overline{q_8^*}) \\
&\quad - \int_{\theta=-\tau_M}^{0}\int_{\xi=0}^{\theta} \frac{1}{\bar\rho}(\overline{q_1^*},\ldots,\overline{q_8^*})\mathrm{e}^{-\mathrm{i}w_c(\xi-\theta)}\,\mathrm{d}\eta(\theta)(q_1,\ldots,q_8)^{\mathrm{T}}\mathrm{e}^{\mathrm{i}w_c\xi}\,\mathrm{d}\xi \\
&= \frac{1}{\bar\rho}(q_1\overline{q_1^*} + \ldots + q_8\overline{q_8^*}) - \int_{\theta=-\tau_M}^{0}\int_{\xi=0}^{\theta}\left[\frac{1}{\bar\rho}(\overline{q_1^*},\ldots,\overline{q_8^*})M_0(q_1,\cdots,q_8)^{\mathrm{T}}\delta(\theta)\mathrm{e}^{\mathrm{i}w_c\theta}\right. \\
&\quad + \frac{1}{\bar\rho}(\overline{q_1^*},\ldots,\overline{q_8^*})M_1(q_1,\ldots,q_8)^{\mathrm{T}}\delta(\theta+\tau_1)\mathrm{e}^{\mathrm{i}w_c\theta} \\
&\quad + \frac{1}{\bar\rho}(\overline{q_1^*},\ldots,\overline{q_8^*})M_2(q_1,\ldots,q_8)^{\mathrm{T}}\delta(\theta+\tau_2)\mathrm{e}^{\mathrm{i}w_c\theta} \\
&\quad + \frac{1}{\bar\rho}(\overline{q_1^*},\ldots,\overline{q_8^*})M_3(q_1,\ldots,q_8)^{\mathrm{T}}\delta(\theta+\tau_3)\mathrm{e}^{\mathrm{i}w_c\theta} \\
&\quad \left. + \frac{1}{\bar\rho}(\overline{q_1^*},\ldots,\overline{q_8^*})M_4(q_1,\ldots,q_8)^{\mathrm{T}}\delta(\theta+\tau_4)\mathrm{e}^{\mathrm{i}w_c\theta}\right]\mathrm{d}\xi\,\mathrm{d}\theta \\
&= \frac{1}{\bar\rho}[(q_1\overline{q_1^*}\ldots + q_8\overline{q_8^*}) + J_1\tau_1\mathrm{e}^{-\mathrm{i}w_c\tau_1} + J_2\tau_2\mathrm{e}^{-\mathrm{i}w_c\tau_2} + J_3\tau_3\mathrm{e}^{-\mathrm{i}w_c\tau_3} + J_4\tau_4\mathrm{e}^{-\mathrm{i}w_c\tau_4}] \\
&= 1.
\end{aligned}$$

Hence $\bar\rho$ is determined to be (3.29).

Appendix B.

From $g(z,\bar{z}) = \overline{q^*}^{\mathrm{T}}(0)G_0(\mathbb{X}_t)$, we compute

$$g(z,\bar{z}) = \frac{1}{\bar{\rho}}(\overline{q_1^*},\ldots,\overline{q_8^*})\cdot \begin{pmatrix} m_{11}x_{2,t}^2(-\tau_1)+m_{12}x_{2,t}(-\tau_1)y_{4,t}(-\tau_1)+m_{13}y_{4,t}^2(-\tau_1)+m_{14}x_{2,t}^3(-\tau_1) \\ +m_{15}x_{2,t}^2(-\tau_1)y_{4,t}(-\tau_1)+m_{16}x_{2,t}(-\tau_1)y_{4,t}^2(-\tau_1)+m_{17}y_{4,t}^3(-\tau_1)+\text{h.o.t.} \\ 0 \\ m_{31}x_{2,t}^2(-\tau_3)+m_{32}x_{2,t}^3(-\tau_3)+\text{h.o.t.} \\ 0 \\ m_{51}y_{2,t}^2(-\tau_1)+m_{52}y_{2,t}(-\tau_1)x_{4,t}(-\tau_1)+m_{53}x_{4,t}^2(-\tau_1)+m_{54}y_{2,t}^3(-\tau_1) \\ +m_{55}y_{2,t}^2(-\tau_1)x_{4,t}(-\tau_1)+m_{56}y_{2,t}(-\tau_1)x_{4,t}^2(-\tau_1)+m_{57}x_{4,t}^3(-\tau_1)+\text{h.o.t.} \\ 0 \\ m_{71}y_{2,t}^2(-\tau_3)+m_{72}y_{2,t}^3(-\tau_3)+\text{h.o.t.} \\ 0 \end{pmatrix}.$$

By (3.31) and (3.32), we obtain

$$\mathbb{X}_t(\theta) = zq(\theta)+\overline{zq(\theta)}+W_{20}(\theta)\frac{z^2}{2}+W_{11}(\theta)z\bar{z}+W_{02}(\theta)\frac{\bar{z}^2}{2}+\cdots.$$

It turns out that, for $k,\ j=1,2,3,4$,

$$\begin{aligned} x_{k,t}(-\tau_j) &= zq_k e^{-\mathrm{i}w_c\tau_j}+\bar{z}\bar{q}_k e^{\mathrm{i}w_c\tau_j}+W_{20}^{(k)}(-\tau_j)\frac{z^2}{2}+W_{11}^{(k)}(-\tau_j)z\bar{z}+W_{02}^{(k)}(-\tau_j)\frac{\bar{z}^2}{2} \\ &\quad +o(|(z,\bar{z})|^3), \\ y_{k,t}(-\tau_j) &= zq_{k+4}e^{-\mathrm{i}w_c\tau_j}+\bar{z}\bar{q}_{k+4}e^{\mathrm{i}w_c\tau_j}+W_{20}^{(k+4)}(-\tau_j)\frac{z^2}{2}+W_{11}^{(k+4)}(-\tau_j)z\bar{z}+W_{02}^{(k+4)}(-\tau_j)\frac{\bar{z}^2}{2} \\ &\quad +o(|(z,\bar{z})|^3), \end{aligned}$$

where $W_{20}^{(k)}(\theta)$, $W_{11}^{(k)}(\theta)$ and $W_{02}^{(k)}(\theta)$ are the kth components of $W_{20}(\theta)$, $W_{11}(\theta)$ and $W_{02}(\theta)$, respectively. Hence, we obtain g_{20}, g_{11}, g_{02} and g_{21}.

Appendix C.

We compute $W_{20}(\theta)$ and $W_{11}(\theta)$. By (3.31),

$$\begin{aligned} \dot{W} &:= \partial W/\partial t(t,\theta) \\ &= \dot{\mathbb{X}}_t - \dot{z}q(\theta)-\dot{\bar{z}}\bar{q}(\theta) \\ &= A\mathbb{X}_t+R_0\mathbb{X}_t-[\mathrm{i}w_c z+\overline{q^*}^{\mathrm{T}}(0)f_0(z,\bar{z})]q(\theta)-[-\mathrm{i}w_c\bar{z}+q^*(0)^{\mathrm{T}}\overline{f_0}(z,\bar{z})]\bar{q}(\theta) \\ &= A\mathbb{X}_t+R_0\mathbb{X}_t-Azq-A\bar{z}\bar{q}-2\mathrm{Re}(\overline{q^*}^{\mathrm{T}}(0)f_0(z,\bar{z})q(\theta)) \\ &= AW-2\mathrm{Re}(\overline{q^*}^{\mathrm{T}}(0)f_0(z,\bar{z})q(\theta))+R_0\mathbb{X}_t \\ &= \begin{cases} AW-2\mathrm{Re}(\overline{q^*}^{\mathrm{T}}(0)f_0(z,\bar{z})q(\theta)), & \theta\in[-\tau_M,0), \\ AW-2\mathrm{Re}(\overline{q^*}^{\mathrm{T}}(0)f_0(z,\bar{z})q(\theta))+f_0(z,\bar{z}), & \theta=0, \end{cases} \\ &=: AW+H(z,\bar{z},\theta). \end{aligned} \tag{6.1}$$

We expand $H(z,\bar{z},\theta)$ as

$$H(z,\bar{z},\theta) = H_{20}(\theta)\frac{z^2}{2}+H_{11}(\theta)z\bar{z}+H_{02}(\theta)\frac{\bar{z}^2}{2}+\cdots. \tag{6.2}$$

Next, taking the derivative of W with respect to t in (3.32), we obtain

$$\dot{W} = W_z\dot{z} + W_{\bar{z}}\dot{\bar{z}}. \tag{6.3}$$

Substituting (3.32) and (3.33) into (6.3), we obtain

$$\dot{W} = (W_{20}(\theta)z + W_{11}(\theta)\bar{z} + \cdots)(\mathrm{i}w_c z + g) + (W_{11}(\theta)z + W_{02}(\theta)\bar{z} + \cdots)(-\mathrm{i}w_c\bar{z} + \bar{g}). \tag{6.4}$$

On the other hand, by (3.32), (6.1) and (6.2), we have

$$\dot{W} = (AW_{20}(\theta) + H_{20}(\theta))\frac{z^2}{2} + (AW_{11}(\theta) + H_{11}(\theta))z\bar{z} + (AW_{02}(\theta) + H_{02}(\theta))\frac{\bar{z}^2}{2} + \cdots. \tag{6.5}$$

Comparing the coefficients with (6.4) and (6.5), we obtain

$$AW_{20}(\theta) - 2\mathrm{i}w_c W_{20}(\theta) = -H_{20}(\theta), \tag{6.6}$$
$$AW_{11}(\theta) = -H_{11}(\theta). \tag{6.7}$$

Recall that $H(z,\bar{z},\theta) = -2\mathrm{Re}(\overline{q^*}^{\mathrm{T}}(0)f_0(z,\bar{z})q(\theta)) + R_0\mathbb{X}_t = -g(z,\bar{z})q(\theta) - \overline{g(z,\bar{z})}\bar{q}(\theta) + R_0\mathbb{X}_t$, cf (3.33) and (6.1). Thanks to (3.34), we derive

$$\begin{aligned} H(z,\bar{z},\theta) = &-(\tfrac{1}{2}g_{20}z^2 + g_{11}z\bar{z} + \tfrac{1}{2}g_{02}\bar{z}^2 + \cdots)q(\theta) \\ &-(\tfrac{1}{2}\bar{g}_{20}\bar{z}^2 + \bar{g}_{11}\bar{z}z + \tfrac{1}{2}\bar{g}_{02}z^2 + \cdots)\bar{q}(\theta) + R_0\mathbb{X}_t. \end{aligned} \tag{6.8}$$

Comparing the coefficients in (6.2) with (6.8), we obtain, for $-\tau_M \leqslant \theta < 0$,

$$H_{20}(\theta) = -g_{20}q(\theta) - \bar{g}_{02}\bar{q}(\theta), \tag{6.9}$$
$$H_{11}(\theta) = -g_{11}q(\theta) - \bar{g}_{11}\bar{q}(\theta). \tag{6.10}$$

Recall the definition of A in (3.24), and substitute (6.9) and (6.10) into (6.6) and (6.7) respectively, we obtain (3.36). Obviously, for $-\tau_M \leqslant \theta < 0$, the solution of (3.36) is (3.37). In the following, we shall find the matrices E_1 and E_2 to establish $W_{20}(\theta)$ and $W_{11}(\theta)$.

From (6.6), (6.7) and the definition of A in (3.24), we have

$$AW_{20}(0) = \int_{-\tau_M}^{0} \mathrm{d}\eta(\theta,0)W_{20}(\theta) = 2\mathrm{i}w_c W_{20}(0) - H_{20}(0), \tag{6.11}$$
$$AW_{11}(0) = \int_{-\tau_M}^{0} \mathrm{d}\eta(\theta,0)W_{11}(\theta) = -H_{11}(0). \tag{6.12}$$

Since $H(z,\bar{z},0) = -g(z,\bar{z})q(0) - \overline{g(z,\bar{z})}\bar{q}(0) + R_0\mathbb{X}_t(0) = -g(z,\bar{z})q(0) - \overline{g(z,\bar{z})}\bar{q}(0) + G_0(\mathbb{X}_t)$, we have

$$H_{20}(0) = -g_{20}q(0) - \bar{g}_{02}\bar{q}(0) + \tilde{E}_1,$$
$$H_{11}(0) = -g_{11}q(0) - \bar{g}_{11}\bar{q}(0) + \tilde{E}_2,$$

where

$$\tilde{E}_1 = \begin{pmatrix} 2e^{-2iw_c\tau_1}(m_{11}q_2^2 + q_8(m_{12}q_2 + m_{13}q_8)) \\ 0 \\ 2e^{-2iw_c\tau_3}m_{31}q_2^2 \\ 0 \\ 2e^{-2iw_c\tau_1}(m_{53}q_4^2 + q_6(m_{52}q_4 + m_{51}q_6)) \\ 0 \\ 2e^{-2iw_c\tau_3}m_{71}q_6^2 \\ 0 \end{pmatrix},$$

$$\tilde{E}_2 = \begin{pmatrix} 2m_{11}|q_2|^2 + 2m_{12}\mathrm{Re}(q_8\bar{q}_2) + 2m_{13}|q_8|^2 \\ 0 \\ 2m_{31}|q_2|^2 \\ 0 \\ 2m_{53}|q_4|^2 + 2m_{52}\mathrm{Re}(q_6\bar{q}_4) + 2m_{51}|q_6|^2 \\ 0 \\ 2m_{71}|q_6|^2 \\ 0 \end{pmatrix}.$$

Moreover, from (3.27), we derive

$$\left(iw_c I - \int_{-\tau_M}^{0} e^{iw_c\theta}\, d\eta(\theta, 0)\right) q(0) = 0, \tag{6.13}$$

$$\left(-iw_c I - \int_{-\tau_M}^{0} e^{-iw_c\theta}\, d\eta(\theta, 0)\right) \bar{q}(0) = 0. \tag{6.14}$$

By (6.13) and (6.14), we can rewrite (6.11) and (6.12) as

$$\left(2iw_c I - \int_{-\tau_M}^{0} e^{2iw_c\theta}\, d\eta(\theta, 0)\right) E_1 = \tilde{E}_1,$$

$$-\int_{-\tau_M}^{0} d\eta(\theta, 0) E_2 = \tilde{E}_2.$$

Hence, we obtain (3.38) and (3.39). We then substitute (3.38) and (3.39) into (3.37) to obtain $W_{20}(\theta)$ and $W_{11}(\theta)$.

References

[1] Baker R E, Schnell S and Maini P K 2006 A mathematical investigation of a clock and wavefornt model for somitogenesis *J. Math. Biol.* **52** 458–82

[2] Campanelli M and Gedeon T 2010 Somitogenesis clock-wave initiation requires differential decay and muptiple binding sites for clock protein *PLoS Comput. Biol.* **6** e1000728

[3] Campbell S A, Ncube I and Wu J 2006 Multistability and stable asynchronous periodic oscillations in a multiple-delayed neural system *Physica* D **214** 101–19

[4] Cinquin O 2007 Repressor dimerization in the zebrafish somitogenesis clock *PLoS Comput. Biol.* **3** 293–303

[5] Cooke J and Zeeman E C 1976 A clock and wavefront model for control of the number of repeated structures during animal morphogenesis *J. Theor. Biol.* **58** 455–76

[6] Dequéant M L, Glynn E, Gaudenz K, Wahl M, Chen L, Mushegian A and Pourqué O 2006 A complex oscillating network of signaling genes underlies the mouse segmentation clock *Science* **314** 1595–8

[7] Dubrulle J, McGrew M J and Pourquié O 2001 FGF signaling controls somite boundary position and regulates segmentation clock control of spatiotemporal Hox gene activation *Cell* **106** 219–32

[8] Dubrulle J and Pourquié O 2002 From head to tail: links between the segmentation clock and antero-posterior patterning of the embryo *Curr. Opin. Genet. Dev.* **12** 519–23

[9] Dubrulle J and Pourquié O 2004 fgf8 mRNA decay establishes a gradient that couples axial elongation to patterning in the vertebrate embryo *Nature* **427** 419–22
[10] Feng P and Navaratna M 2007 Modelling periodic oscillations during somitogenesis *Math. Biosc.* **4** 661–73
[11] Giudicelli F and Lewis J 2004 The vertebrate segmentation clock *Curr. Opin. Genet. Dev.* **14** 407–14
[12] Giudicelli F, Özbudak E M, Wright G J and Lewis J 2007 Setting the tempo in development: an investigation of the zebrafish somite clock mechanism *PLOS Biol.* **5** e150 1309–23
[13] Goldbeter A and Pourquié O 2008 Modeling the segmentation clock as a network of coupled oscillations in the Notch, Wnt and FGF signaling pathways *J. Theor. Biol.* **252** 574–85
[14] Golubitsky M, Schaeffer D G and Stewart I 1988 *Singularities and Groups in Bifurcation Theory* (New York: Springer)
[15] Hassard B D, Kazarinoff N D and Wan Y H 1981 *Theory and Applications of Hopf Bifurcation* (Cambridge: Cambridge University Press)
[16] Herrgen L, Ares S, Morelli L G, Schröter C, Jülicher F and Oates A C 2010 Intercellular coupling regulates the period of the segmentation clock *Curr. Biol.* **20** 1244–53
[17] Holley S A 2007 The genetics and embryology of zebrafish metamerism *Dev. Dyn.* **236** 1422–49
[18] Jiang Y J, Aerne B L, Smithers L, Haddon C, Ish-Horowicz D and Lewis J 2000 Notch signaling and the synchronization of the somite segmentation clock *Nature* **408** 475–9
[19] Kawamura A, Koshida S, Hijikata H, Sakaguchi T, Kondoh H and Takada S 2005 Zebrafish hairy/enhancer of split protein links FGF signaling to cyclic gene expression in the periodic segmentation of somites *Genes Dev.* **19** 1156–61
[20] Krawcewicz W and Wu J 1999 Theory and applications of Hopf bifurcations in symmetric functional-differential equations *Nonlinear Anal.* **35** 845–70
[21] Lewis J 2003 Autoinhibition with transcriptional delay: a simple mechanism for the zebrafish somitogenesis oscillator *Curr. Biol.* **13** 1398–408
[22] Lewis J, Hanisch A and Holder M 2009 Notch signaling, the segmentation clock, and the patterning of vertebrate somites *J. Biol.* **8** 44
[23] Liao K L and Shih C W 2012 A lattice model on somitogenesis of zebrafish, submitted
[24] Morelli L G, Ares S, Herrgen L, Schröter C, Jülicher F and Oates A C 2009 Delayed coupling theory of vertebrate segmentation *HFSP* **3** 55–66
[25] Özbudak E M and Lewis J 2008 Notch signalling synchronizes the zebrafish segmentation clock but is not needed to create somite boundaries *PLoS Genet.* **4** e15
[26] Pourquié O 2001 The vertebrate segmentation clock *J. Anat.* **199** 169–75
[27] Pourquié O 2003 The segmentation clock:converting embryonic time into spatial pattern *Science* **301** 328–30
[28] Riedel-Kruse I H, Müller C and Oates A C 2007 Synchrony dynamics during initiation, failure, and rescue of the segmentation clock *Science* **317** 1911–5
[29] Rodríguez-González J G, Santillán M, Fowler A C and Mackey M C 2007 The segmentation clock in mice: interaction between the Wnt and Notch signalling pathways *J. Theor. Biol.* **248** 37–47
[30] Shih C W and Tseng J P 2008 Convergent dynamics for multistable delayed neural networks *Nonlinearity* **21** 2361–89
[31] Shih C W and Tseng J P 2011 Global synchronization and asymptotic phases for a ring of identical cells with delayed coupling *SIAM J. Math. Anal.* **43** 1667–97
[32] Sieger D, Ackermann B, Winkler C, Tautz D and Gajewski M 2006 her1 and her13.2 are jointly required for somitic border specification along the entire axis of the fish embryo *Dev. Biol.* **293** 242–51
[33] Uriu K, Morishita Y and Iwasa Y 2009 Traveling wave formation in vertebrate segmentation *J. Theor. Biol.* **257** 385–96
[34] Uriu K, Morishita Y and Iwasa Y 2010 Synchronized oscillation of the segmentation clock gene in vertebrate development *J. Math. Biol.* **61** 207–29
[35] Uriu K, Morishita Y and Iwasa Y 2010 Random cell movement promotes synchronization of the segmentation clock *Proc. Natl Acad. Sci. USA* **107** 4979–84
[36] Wan A and Zou X 2009 Hopf bifurcation analysis for a model of genetic regulatory system with delay *J. Math. Anal. Appl.* **356** 464–76
[37] Wei J and Yu C 2009 Hopf bifurcation analysis in a model of oscillatory gene expression with delay *Proc. R. Soc. Edinb.* A **139** 879–95
[38] Wahl M B, Deng C, Lewandoski M and Pourquié O 2007 FGF signaling acts upstream of the NOTCH and WNT signaling pathways to control segmentation clock oscillations in mouse somitogenesis *Development* **134** 4033–41
[39] Wu J 1998 Symmetric functional differential equations and neural networks with memory *Trans. Am. Math. Soc.* **350** 4799–838